Review Article

RADIATION SHIELDING TECHNOLOGY

J. Kenneth Shultis and Richard E. Faw*

Abstract—**An historical review of the development of shielding techniques for indirectly ionizing radiation is presented, along with a summary of techniques at various levels of sophistication for shielding design and analysis.**
Health Phys. 88(4):297–322; 2005

Key words: reviews; shielding; historical profiles; Health Physics Society

INTRODUCTION

THIS IS a review of the technology of shielding against the effects of indirectly ionizing x rays, gamma rays, and neutrons produced by sources of commercial, industrial, and military concern. Not addressed is shielding for radiation sources used exclusively for medical applications and sources associated with high-energy charged-particle accelerators.

There are two parts to the review. The first treats the evolution of radiation-shielding technology from the beginning of the 20th century, when radium emanations and low energy x rays were the only concerns and design methods were primitive, to the beginning of the 21st century, when radiation shielding needs are very diverse and when computational technology gives broad rein to design methods. The second part of the review addresses the foundations of radiation shielding analysis and design, with emphasis on the characterization of radiation sources and radiation fields, the transport of radiation through matter, and the conversion of radiation intensities into radiation doses meaningful in the assessment of risk.

An extensive bibliography is provided in an effort to address both documents of historical interest and documentation of the state-of-the-art of photon and neutron shielding. For historical documentation, the authors are indebted to Goldstein's 1967 tribute to Everitt Blizard, to Schaeffer's text and his own historical review (1973), to Taylor's review of the work of the NCRP and the ICRP (1979), and to experiences related by Simpson (1995) and Rockwell (2004).

As compilers of this review, we have tried to be objective in our selection of topics. Clearly, we could not acknowledge all the many contributors to the advance of radiation transport theory and radiation shielding design and analysis, much less the entire body of published work. An historical review, like beauty, is in the eye of the beholder. Our eyes were opened to this field in the late 1950's, and we can't comment at first hand to earlier work. Those whose work we recognize are mostly those whose work intersected in some way with our own. To those we may have slighted, we offer not only our apologies but also our thanks. Radiation shielding design and analysis has become a mature discipline with foundations established over many decades by many persons, all of whom can take pride in their contributions.

HISTORY OF RADIATION SHIELDING

The early years

Shielding of x-ray generators. The hazards of x rays were recognized within months of Roentgen's 1895 discovery, but dose limitation by time, distance, and shielding was at the discretion of the individual practitioner until about 1913. Only then were there organized professional efforts to establish guides for radiation protection, and not until about 1925 were there instruments available to quantify radiation exposure. In his monumental survey of organization for radiation protection, Taylor (1979) begins with British and German efforts at establishing guidance for x-ray shielding. In 1913, the German Radiological Society on X-Ray Protection Measures issued recommendations that 2 mm of lead shielding was needed, regardless of generator voltage, workload, or filtration. In Britain, the Roentgen Society addressed radiation protection, stressing operator protection, the need for beam collimation, and the importance of scattered x rays. No explicit recommendations on shielding requirements were issued.

* Department of Mechanical and Nuclear Engineering, Kansas State University, Manhattan, KS 66506.

For correspondence or reprints contact: J. K. Shultis at the above address, or email at jks@ksu.edu.

(*Manuscript received* 25 *September* 2004; *accepted* 9 *December* 2004)

0017-9078/05/0

In 1921, the British X-Ray and Radium Protection Committee issued broad guidelines, both physical and administrative, on radiation protection in x-ray facilities. For diagnostic examinations, 2 mm of lead screening was recommended for the operator, as well as gloves with effectively 0.5 mm of lead shielding. For superficial therapy (up to 100 kV x rays), 2 mm of lead shielding was recommended. For deep therapy (in excess of 100 kV x rays) 3 mm of lead shielding was recommended. Again, filtration and workload were not addressed.

Mutscheller (1925) introduced important concepts in x-ray shielding. He expressed the erythema dose,[†] *ED*, quantitatively in terms of the beam current i (mA), exposure time t (min), and source-to-receiver distance r (m), namely,

$$ED = 0.00368\frac{it}{r^2} \quad (1)$$

independent of x-ray energy. Years later, as observed by Taylor (1981), unit erythema dose was equated to an exposure X of about 600 R. Thus, in modern terms,

$$X = K_o\frac{it}{r^2} \simeq 2.2\frac{it}{r^2}. \quad (2)$$

Mutscheller also published attenuation factors in lead as a function of lead thickness and x-ray average wavelength. This is the standard approach for assessment of x-ray exposure rates, with K_o taking on values of 0.24 to 0.97 R m^2 mA^{-1} min^{-1} for well-filtered x-rays with peak energies ranging from 30 to 140 kV (Simpkin 1987, 1989).

Evolutionary changes in shielding recommendations were made during the decades preceding World War II. These included consideration of scattered x rays, refinements in shielding requirements in terms of x-ray tube voltages, recommendations for use of goggles (0.25-mm lead equivalent) and aprons (0.5-mm lead equivalent) for fluoroscopy, and specifications for tube-enclosure shielding and structural shielding for control rooms.

In the United States, the Advisory Committee on X-Ray and Radium Protection was established in 1929, under the auspices of the National Bureau of Standards. In 1964, the Committee was congressionally chartered as the National Council on Radiation Protection and Measurements (NCRP). NCRP Reports 1 and 3 were issued in 1931 and 1936. The former recommended a tolerance dose of 0.2 R per day, the second 0.1 R per day for occupational exposure.

For additional information on the history of x-ray shielding, the reader is referred to excellent reviews published by this journal. Archer (1995) addresses diagnostic x-ray installations; McGinley and Miner (1995) address the shielding of therapeutic x-ray installations. For more information on the organizational aspects of x-ray shielding, the reader is referred to the aforementioned compendium and article by Taylor (1979, 1981).

Shielding of radium sources. In 1927, the International Committee on X-Ray and Radium Protection issued the following recommendations for storage of radium sources. Tubes and applicators should have at least 5 cm of lead shielding per 100 mg of radium. Radium solutions required lead shielding ranging from 15 cm for a 0.5 g source to 30 cm for a 2 g source. NCRP Report 2 (1934) specified a 3-m protective zone around stored Ra sources, and recommended exhaust fans or hoods for removal of radon and decay products escaping from unsealed sources. Shielding of stored sources was revised to 4 cm of lead for 100 mg to 6 cm for 300 mg. NCRP Report 4 (1938) addressed dosimetry for gamma rays emitted from radium sources. It was not until 1941 that there was established a tolerance dose for radium, expressed in terms of a maximum permissible body burden of 0.1 μCi. This was done largely in consideration of the experiences of early "radium-dial" painters and the need for standards on safe handling of radioactive luminous compounds (NCRP 1941).

Manhattan Project and early postwar period

Wartime. During World War II, research on nuclear fission, construction of nuclear reactors, production of enriched uranium, generation of plutonium and separating it from fission products, and the design, construction, testing, and deployment of nuclear weapons—all were accomplished at breakneck speed in the Manhattan Project. The project was a scientific, engineering, management, and construction project of extraordinary magnitude and success. The pace of the project and the introduction of many new and dangerous materials and processes demanded much of industrial hygiene. Radiation sources new in type and magnitude demanded not only protective measures such as shielding but also examination of biological effects and establishment of work rules.

Jones (1985) describes health and safety programs within the Manhattan Engineering District. In June 1943, a medical section was established at District headquarters under the direction of Professor Stafford Warren. Medical research programs were established to address issues such as metabolism and dosimetry for ingested or inhaled radionuclides. Industrial hygiene programs were established to deal with many new and hazardous substances

[†] An ED value of unity represents a combination of time, distance, and beam current just leading to a first-degree burn.

such as plutonium and uranium hexafluoride. What we might call operational health physics got its start. Mining, milling, processing and enriching uranium involved new risks. Processing spent fuel from nuclear reactors, dealing with waste fission and activation products, and extracting actinides also involved new risks. Bomb development required dealing with radiation risks as well as risks of high explosives. These health and safety efforts were very successful. The Manhattan Engineering District operated with occupational injury rates much less than those for comparable private industry.

Uncertainties in radiation transport made shielding design very conservative. Shielding for the 1943 graphite-moderated reactor in Chicago, constructed of concrete and paraffinized wood and based on attenuation measurements made by Fermi and Zinn, was adequate for gamma rays and over designed for neutrons (Schaeffer 1973). After this reactor operated successfully, the X-10 reactor was built at what would become the Oak Ridge National Laboratory to provide data for the design of plutonium-production reactors. The X-10 reactor was constructed of graphite and was air cooled. Its shielding was 2.1-m-thick made of baryte and haydite concretes, baryte being of high density and haydite being high in hydrogen content. This shielding also was adequate for gamma rays and over designed for neutrons (Schaeffer 1973; Jaeger 1975). Operation of the X-10 reactor revealed problems with streaming of gamma rays and neutrons around access holes in the shield. The water-cooled graphite plutonium production reactors at Hanford, Washington, used iron thermal shields and high density limonite and magnetite concrete biological shields. Concrete compositions and design methods are discussed in the Engineering Compendium on Radiation Shielding (Jaeger 1975) and in National Standards (ANS 1997).

By the 1940's, the importance of scattered gamma rays was certainly known from measurements, and use of the term *buildup factor* to characterize the relative importance of scattered and unscattered gamma rays had its origin during the days of the Manhattan Project (Goldstein 1959). Neutron diffusion theory and Fermi age theory were established, but shielding requirements for high-energy neutrons were not well understood. Wartime radiation shielding was an empirical, rule-of-thumb craft (Goldstein 1967).

Nuclear reactors for propulsion. The Atomic Energy Act of 1946 transferred control of nuclear matters from the Army to the civilian Atomic Energy Commission (AEC). That same year, working with the AEC, the U.S. Navy began development of a nuclear powered submarine and the U.S. Air Force a nuclear powered aircraft. Both of these enterprises demanded minimization of space and weight of the nuclear reactor power source. Such could be accomplished only by minimizing design margins and that required knowledge of mechanical, thermal, and nuclear properties of materials with greater precision than known before. Goldstein (1967) and Schaeffer (1973) describe how the challenge was taken up in 1947 at Oak Ridge National Laboratory under the direction of Everitt Blizard in the first organized research program in nuclear reactor shielding. The X-10 graphite reactor had a 2-ft square aperture in its shielding from which a neutron beam could be extracted, the intensity being augmented by placement of fuel slugs in front of the aperture. Attenuation of neutrons could then be measured within layers of shielding materials placed against the beam aperture. Early measurements revealed the importance of capture gamma rays produced when neutrons were absorbed. Improved experimental geometry was obtained by using a converter plate instead of relying on fission neutrons from fuel slugs. The converter plate was a thin plate, in effect a plane of well defined shape (disk or rectangle), containing enriched uranium. A broadly uniform beam of thermal neutrons incident on the plate generated a well-defined source of fission neutrons. C.E. Clifford then set up a water tank adjacent to the fission source, with shielding slabs and instrumentation within the tank. This Lid Tank Shielding Facility, LTSF, was the precursor of many so-called bulk shielding facilities incorporated into many water-cooled research reactors. Early among these was the LTSF at Brookhaven National Laboratory, the Bulk Shield Reactor at Oak Ridge National Laboratory, and the British bulk-shielding reactor LIDO, completed in 1956. The British research reactor BEPO, similar to the X-10 reactor, began operation in 1948.

Streaming of radiation through shield penetrations and heating in concrete shields due to neutron and gamma-ray absorption were early shielding studies conducted in support of gas-cooled reactor design. This work is described in the text by Price et al. (1957). Additional efforts were undertaken soon thereafter at universities as well as government and industrial laboratories. Shielding material properties, neutron attenuation, the creation of capture and inelastic scattering gamma rays, reflection and streaming of neutrons and gamma rays through ducts and passages, and radiation effects on materials were major research topics.

Although a nuclear-powered aircraft never took flight, the wealth of information gained on the thermal, mechanical, and shielding properties of many special materials is a valuable legacy. Development of a nuclear-powered aircraft required examination of the relative importance of shielding the reactor and the crew compartment. It was also necessary to perform measurements

absent ground reflection or in such a way as to allow correction for such reflection. This was accomplished in several ways. According to Schaeffer (1973), a ground test reactor was suspended by crane for tests of ground reflection. Then an aircraft shield test reactor was flown in the bomb-bay of a B-36 aircraft to allow measurements at altitude. The Oak Ridge tower shielding facility went into operation in 1954, and remained in operation for almost 40 y. Designed for the aircraft nuclear propulsion program, the facility allowed suspension of a reactor hundreds of feet above grade and separate suspension of aircraft crew compartments. In its long life, the TSF also supported nuclear defense and space nuclear applications.

The decade of the 1950's

This era saw the passage in the U.S. of the Atomic Energy Act of 1954, the Atoms for Peace program, and the declassification of nuclear data. Advances in neutron shielding technology came together in the treatment of neutron attenuation in hydrogenous media. Advances in gamma-ray transport methodology permitted calculation of buildup factors for treatment of scattered photons. All these technological advances enabled design work for nuclear reactors to proceed well before widespread use of digital computers. The NERVA program (nuclear energy for rocket vehicle applications) began in 1955 under the sponsorship of NASA and the Atomic Energy Commission. The first nuclear rocket (KIWI) was tested in 1959. The Atmospheric Nuclear Test Ban Treaty of 1963 prevented the deployment of a nuclear rocket system and the program was ended in 1972. Atmospheric testing of nuclear weapons continued through the decade, with the U.S. testing a fusion device in November 1952 and the USSR in August 1953. The first experimental breeder reactor, EBR-I, was operational and generated electricity in December 1951, construction having begun in May 1949. Construction of the first commercial nuclear power plant, Shippingport, was begun in 1954 and power generation commenced in December 1957.

Advances in neutron shielding methods. These advances resulted from measurements at the LTSF and other bulk-shielding facilities. One advancement was the measurement of point kernels, or Green's functions, for attenuation of fission neutrons in water. The other was the discovery that the effect of water-bound oxygen, indeed the effect of homogeneous or heterogeneous shielding materials in hydrogenous media, could be modeled by exponential attenuation governed by effective "removal" cross sections for the non-hydrogen components.

Because the hydrogen cross section increases with decreasing fast-neutron energies, Albert and Welton (1950) recognized the first scatter with hydrogen, on average, results in a large energy loss for very energetic and very penetrating fission neutrons, which are then very quickly removed from the fast energy region by the now much more probable scattering interactions with hydrogen. Thus, the first scatter with hydrogen effectively removes the neutron from the fast energy region. In an hydrogenous medium, fission-neutron attenuation hence could be treated as attenuation in hydrogen superimposed with energy-independent absorption, i.e., removal from the fast energy region by the non-hydrogen components. Albert and Welton determined that the total uncollided fast-neutron flux density should vary with distance r from a point source of fission neutrons in water as

$$\phi(r) \propto \frac{r^{\gamma/2}}{4\pi r^2} \exp(-\alpha r^{\gamma}) \exp(-\mu_{R,O} r). \qquad (3)$$

Here the constants α and γ are based on empirical approximations for the energy spectrum of fission neutrons and the energy-dependent scattering cross section for hydrogen, and take on values 0.928 and 0.58, respectively, for fission neutrons produced by thermal fission of ^{235}U. The exponential-attenuation term, in which $\mu_{R,O}$ is called the macroscopic *removal* cross section for oxygen, accounts simply and entirely for the effect of oxygen on fast-neutron attenuation, and empirically has the value 0.0308 cm^{-1} for water at density 1 g cm^{-3}. The corresponding microscopic removal cross section is $\sigma_{R,O}$ = 0.921 b. This formula, and the Casper formula to follow, are easily modified to apply to hydrogenous media other than water, to account for different hydrogen atomic densities, and to account for neutron removal by elements or compounds other than oxygen. Many removal cross sections were measured by Chapman and Storrs (1955) using the LTSF at Oak Ridge National Laboratory. Selected values are given in Table 1.

In 1960, Casper published the following point-kernel equation for fast-neutron absorbed dose in tissue due to a point ^{235}U fission source in water:

Table 1. Selected removal cross sections[a]

Material	σ_r (b/atom)
Aluminum	1.31 ± 0.05
Beryllium	1.07 ± 0.06
Carbon	0.81 ± 0.05
Iron	1.98 ± 0.08
Lead	3.53 ± 0.30
Oxygen	0.99 ± 0.10
Uranium	3.6 ± 0.4

[a] Source: Chapman and Storrs (1955).

$$G_{H_2O}(r) = \frac{5.39 \times 10^{-11}}{4\pi r^2} r^{0.349} \exp(-0.422 r^{0.698} - 0.0308 r), \quad (4)$$

where r has units of centimeters and G has units of Gy for a source strength of one fission neutron. Suppose that there is a point fission source surrounded by a fixed shield of thickness t composed of a material with removal cross section μ_r followed by water of thickness r. Then, provided that r is at least 50 cm, the absorbed dose, per fission neutron, is given by

$$D = \frac{r^2}{(r+t)^2} G_{H_2O}(r) e^{-\mu_R t}. \quad (5)$$

Advances in gamma-ray shielding methods. As the decade began, a major program at the National Bureau of Standards was underway in research on electron and photon transport (Spencer and Fano 1951). The photon transport effort is described by Fano et al. (1959). Much of the effort dealt with the moments method of solving the transport equation describing the spatial, energy, and angular distributions of particle fluences arising from fixed sources. The method applies to infinite homogeneous media, with well defined monoenergetic sources such as point or infinite-plane isotropic sources. The angular dependence of the particle fluence, $\Phi(\mathbf{r},E,\mathbf{\Omega})$, is expressed as a Legendre polynomial expansion, each term of which is expressed in terms of spatial moments. The energy dependence of each moment is then determined numerically based on attenuation and scattering properties of the medium. Then the process may be reversed, yielding the energy spectrum of the angular distribution of the fluence, or an integral over the energy spectrum, weighted by a fluence-to-dose conversion factor $R(E)$, yielding the angular distribution of the dose rate. From these results buildup factors may be obtained. These represent ratios of the total dose $D(\mathbf{r})$, scattered dose $D^s(\mathbf{r})$ plus uncollided dose $D^o(\mathbf{r})$, to that from uncollided particles only, namely,

$$B(\mathbf{r}) \equiv \frac{D(\mathbf{r})}{D^o(\mathbf{r})} = 1 + \frac{D^s(\mathbf{r})}{D^o(\mathbf{r})}. \quad (6)$$

For a monoenergetic source,

$$B(E_o, \mathbf{r}) = 1 + \frac{1}{\Phi^o(\mathbf{r})} \int_0^{E_o} dE \frac{R(E)}{R(E_o)} \Phi^s(\mathbf{r}, E). \quad (7)$$

In this case, the nature of the dose or response is fully accounted for in the ratio $R(E)/R(E_o)$.

In a collaborative effort with the Bureau of Standards, Goldstein and Wilkins (1954) made use of the SEAC digital computer at the Bureau in a thorough evaluation of energy spectra and buildup factors for many materials and a broad range of photon energies.[‡] The results of this collaborative effort, known widely as NYO-3075, served for many years as the prime source of buildup factor data for use in shielding design. The use of buildup factors in shielding design and analysis was greatly facilitated by interpolation methods devised by Taylor (1954), Berger (1956), and Capo (1959). For a given material, for a point isotropic source in an infinite medium, and in terms of the number λ of mean free paths at source energy, these interpolation formulas are, respectively,

$$B(E_o, \lambda) \simeq A e^{-\alpha_1 \lambda} + [1 - A] e^{-\alpha_2 \lambda}, \quad (8)$$

$$B(E_o, \lambda) \simeq 1 + C\lambda e^{D\lambda}, \quad (9)$$

and

$$B(E_o, \lambda) \simeq \sum_{n=0}^{3} \beta_n \lambda^n, \quad (10)$$

in which parameters A, α_1, α_2, C, D, and β_n depend on the material, the photon energy, and, in principle, the nature of the response.

Advances in Monte Carlo computational methods. The Monte Carlo method of simulating radiation transport computationally has its roots in the work of John von Neumann and Stanislaw Ulam at Los Alamos in the 1940's. Neutron transport calculations were performed in 1948 using the ENIAC digital computer, which had commenced operations in 1945. Major advances were made in the 1950's by Kahn (1950), Goertzel and Kalos (1958), and Cashwell and Everett (1959). Berger (1955, 1956) began a Monte Carlo effort at the National Bureau of Standards that thrived for several decades.

The decade of the 1960's

The 1960's saw the technology of nuclear reactor shielding consolidated in several important publications. Blizard and Abbott (1962) edited and released a revision of a portion of the 1955 Reactor Handbook as a separate volume on radiation shielding, recognizing that reactor shielding had emerged from nuclear reactor physics into a discipline of its own. In a similar vein, the first volume of the Engineering Compendium on Radiation Shielding (Jaeger 1968) was published. These two volumes brought together contributions from scores of authors and had a great influence on both practice and education in the field

[‡] Eight energies from 0.5 to 10 MeV and the following materials: free electrons only, water, Al, Fe, Sn, W, Pb and U.

of radiation shielding. Radiation shielding in the context of nuclear plant design was the theme of Hungerford's 1966 review of the design of the sodium-cooled Fermi plant outside Detroit.

This exciting decade also saw the beginning of the Apollo program, continuation of the NERVA program, the deployments in space of SNAP-3, a radioisotope thermoelectric generator in 1961, and SNAP-10A nuclear-reactor power system in 1965. It also saw the Cuban missile crisis in October 1962, and a major increase in the cold-war apprehension about possible use of nuclear weapons. The Apollo program demanded attention to solar-flare and cosmic radiation sources and the shielding of space vehicles. Cold-war concerns demanded attention to nuclear-weapon effects, particularly structure shielding from nuclear-weapon fallout. Reflection of gamma rays and neutrons and their transmission through ducts and passages took on special importance in structure shielding. The rapid growth in access to digital computers allowed introduction of many computer codes for shielding design and fostered advances in solving various approximations to the Boltzmann transport equation for neutrons and gamma rays. Similar advances were made in treating the slowing-down and transport of charged particles.

Space shielding. Data gathered over many years revealed a very complicated radiation environment in space. Two trapped-radiation belts had been found to surround the earth, an inner proton belt and an outer electron belt. Energy spectra and spatial distributions in these belts are determined by the earth's magnetic field and by the solar wind, a plasma of low-energy protons and electrons. The radiations pose a risk to astronauts and to sensitive electronic equipment. Uniform intensities of very high-energy galactic cosmic rays demand charged-particle shielding for protection of astronauts in long duration missions. The greatest radiation risk faced by Apollo astronauts was from solar flare protons and alpha particles with energies as great as 100 MeV for the former and 400 MeV for the latter. As is well known, flares occur in an 11-y cycle. They can be detected in advance by sun-spot observation and by advanced receipt of electromagnetic radiation. The overall subject of space radiation shielding is treated by Haffner (1967). Data needed for shielding calculations were provided by Hubble (1969), Barkas and Berger (1964), and Berger and Seltzer (1964). Shielding methodology is described by Leimdorfer et al. (1967) and Alsmiller (1967). Advances in electron transport theory are described by Zerby and Keller (1967) and Berger and Seltzer (1968).

Structure shielding. Structure shielding against nuclear-weapon fallout required careful examination of the atmospheric transport of gamma rays of a wide range of energies and expression of angular distributions and related data in a manner easily adapted to analysis of structures. There was a need to assess, at points within a structure, the ratio of interior dose rates to that outside the building, called *reduction factors.* Calculations were completed at the National Bureau of Standards by Lewis Spencer (1962) using the moments method of transport calculations which had been used so successfully in calculation of buildup factors. The engineering methodology was developed by Eisenhauer (1964) and rapidly deployed by the Office of Civil Defense for shelter analysis. The body of theoretical, analytical, and experimental support was documented by Spencer et al. (1980).

Of great importance to structure shielding, but also of interest in reactor and plant shielding, was the need to quantify neutron and gamma-ray reflection and streaming through ducts and voids in shields. Advances through the 1960's and early 1970's have been described thoroughly by Selph (1973). The central concept is the particle albedo, defined for a broad parallel beam of monoenergetic particles passing through a non-attenuating medium and striking a thick reflecting half-space at a fixed polar angle ϑ_o measured from a normal to the reflecting surface. If the incident current or flow, measured per unit area in the surface, is $J_o(E_o,\vartheta_o)$ in units, say, cm^{-2} and the energy and angular distribution of the reflected current is $J_r(E, \vartheta, \psi)$ in units, say, cm^{-2} MeV^{-1} sr^{-1} measured at polar angle ϑ and a zimuthal shift ψ, the differential number albedo is defined as

$$\alpha(E_o, \vartheta_o; E, \vartheta, \psi) = \frac{J_r(E, \vartheta, \psi)}{J_o(E_o, \vartheta_o)} = \frac{\cos \vartheta \phi_r(E, \vartheta, \psi)}{\cos \vartheta_o \phi_o(E_o, \vartheta_o)}. \quad (11)$$

For practical purposes, the albedo commonly used is the *dose albedo*, the ratio of the emergent flow per steradian in dose units to that of the incident radiation. With *R(E)* representing the fluence to dose conversion factor, the dose albedo is defined as

$$\alpha_D(E_o, \vartheta_o; \vartheta, \psi) = \frac{\int dER(E) J_r(E, \vartheta, \psi)}{R(E_o) J_o(E_o, \vartheta_o)}. \quad (12)$$

Characterizing neutron albedos is more complicated. For incident fast neutrons, four albedos may be required: one for fast neutrons, one for intermediate energy neutrons,

one for thermal neutrons, and one for capture gamma rays. Early gamma ray albedo measurements were made by Haggmark et al. (1965) and calculations were made by Berger and Doggett (1956), Berger and Raso (1960), and Raso (1963). Early neutron measurements and calculations were made by Wells (1964) and Maerker and Muckenthaler (1965, 1966). Use of albedos in shielding design and analysis requires analytical approximations to albedo data. Contributors for neutron albedos include French and Wells (1963), Coleman et al. (1967), and Song et al. (1969). Contributors for gamma rays include Chilton and Huddleston (1963), Chilton et al. (1965), and Chilton (1967).

Digital computer applications. Radiation transport calculations are by nature very demanding of computer resources. The community of interest in radiation transport and shielding has been served magnificently for more than four decades by the Radiation Safety Information Computational Center (RSICC). Established in 1962 as the Radiation Shielding Information Center (RSIC) at Oak Ridge National Laboratory, RSICC's mission is to provide in-depth coverage of the radiation transport field to meet the needs of the international shielding community. RSICC collects, organizes, evaluates, and disseminates technical information, including software, involving shielding and protection from the radiation associated with fission and fusion reactors, outer space, accelerators, weapons, medical facilities, and nuclear waste management.

The 1960's saw many new "mainframe" computer codes developed and disseminated. Among these codes were gamma-ray "point-kernel" codes such as ISOSHLD (Engle et al. 1966) and QAD (Malenfant 1967), with versions of both still in use after almost four decades. The discrete-ordinates method of solving the Boltzmann transport equation was devised in the 1950's (Carlson 1955) and put into practice in the 1960s in a series of computer codes, DTF (Lathrop 1965), DOT (Mynatt et al. 1969), and ANISN (Engle 1967). The spherical harmonics method of treating neutron spatial and energy distributions in shields was advanced by Shure in one-dimensional P_3 calculations (1964). Progress in Monte Carlo methods advanced in pace with discrete ordinates methods, and the multi-group Monte Carlo code for neutron and gamma ray transport, MORSE, was introduced at the end of the decade (Straker et al. 1970).

The Monte Carlo method has a rich heritage at Los Alamos. Efforts began in 1947, inspired by John von Neumann and Enrico Fermi. As related in the MCNP operating manual issued by the X-5 Monte Carlo Team (2003), a general-purpose particle-transport code MCS was written in 1963. This was followed by the MCN code for three-dimensional calculations written in 1965.

The decade of the 1970's

The Nuclear Non-Proliferation Treaty (NPT) of 1968 and the National Environmental Policy Act (NEPA) of 1969 had major impacts on the radiation-shielding field in the 1970's and succeeding decades. The NPT precluded nuclear fuel reprocessing and led to ever increasing needs for on-site storage of spent fuel at nuclear power plants. NEPA required exhaustive studies of off-site radiation doses around nuclear power plants and environmental impacts of plant operations. Early in the 1970's there were major disruptions in oil supplies caused by the OPEC embargo. The response in the United States was an energy policy that forbade electricity production using oil or natural gas. The result was placement of many orders for nuclear power plants despite NPT and NEPA constraints. In the field of radiation shielding special attention was given to plant design issues such as streaming of neutrons and gamma rays through voids, passageways, and shield penetrations, to operational issues such as fission product inventories in fuels and gamma ray skyshine, particularly associated with ^{16}N sources. The end of the decade was marked by the 28 March 1979 accident at the Three Mile Island, Unit 2 power plant.

Information essential for plant design, fuel management, and waste management is data tracking radionuclide activities in reactor fuel and process streams, and corresponding strengths and energy spectra of sources, including fission products, activation products, and actinides. To accomplish this, the ORIGEN codes were developed at Oak Ridge National Laboratory (Bell 1973; Croff 1980) and the CINDER code was developed at Los Alamos National Laboratory (England et al. 1976). Assessment of radiation doses from airborne beta-particle emitters was one of the motivations for Berger's work on cloud doses (1974). Although the ETRAN Monte Carlo code for electron transport was available at the National Bureau of Standards, work began in the mid 1970's at Sandia Laboratory on the TIGER code and at Stanford Linear Accelerator Center on the EGS code, both for coupled photon and electron transport by the Monte Carlo method. The former evolved to the Integrated Tiger Series (ITS) of codes (Halbleib et al. 1992), the later to the EGS4 code (Nelson et al. 1985).

Design needs brought new attention to buildup factors and to attenuation of broad beams of neutrons and gamma rays. Eisenhauer and Simmons (1975) and Chilton et al. (1980) published definitive tables of buildup factors. Doggett and Bryan (1970) and Fournie

and Chilton (1980) both addressed attenuation of obliquely incident photons, and the former addressed reflection as well. Roussin and Schmidt (1971) and Roussin et al. (1973) addressed transmission of neutrons and secondary gamma rays through shielding barriers. This decade also saw the publication of two important NCRP reports (1971, 1976) dealing with neutron shielding and dosimetry and with design of medical facilities that protected against effects of gamma rays and high energy x rays.

Design and analysis needs also fostered continuing attention to computer codes for criticality and neutron-transport calculations. Lathrop and Brinkley (1970), Hill (1975), Mynatt et al. (1969), Mynatt and Rhoades (1973), and Rhoades et al. (1979) all introduced discrete ordinates transport codes. Advances in Monte Carlo calculations were also made. The MCN code was merged with the MCG code in 1973 to form the MCNG code for treating coupled neutron-photon transport. Another merger took place with the MCP code in 1977, allowing detailed treatment of photon transport at energies as low as 1 keV. This new code was known, then and now, as MCNP.

The 1980's and 1990's

These years saw the consolidation of resources for design and analysis work. In the 1980's, personal computers allowed methods such as point-kernel calculations to be programmed. In the 1990's, personal computers took over from the main-frame computers in even the most demanding shielding design and analysis. Comprehensive sets of fluence-to-dose conversion factors became available for wide spread use. Radionuclide decay data became available in data bases easily used for characterizing sources. Gamma-ray buildup factors were computed with precision and a superb method of data fitting was devised. All these carried point-kernel as well as more advanced shielding methodology to a new plateau.

Data bases. Long a staple in health physics and nuclear engineering, the Table of the Isotopes (Firestone and Shirley 1996), while unsurpassed in documenting energy levels, is difficult to use in characterizing decay data. Kocher (1981) published data for shielding design and analysis that largely supplanted the data of Martin and Blichert-Toft (1970), Dillman and Von der Lage (1975), and Martin (1976). Then a new MIRD compendium (Weber et al. 1989) and ICRP-38 data base (ICRP 1983) became the norms, with the latter especially useful for characterizing low-energy x ray and Auger electron emission. A wealth of nuclear structure and decay data is available from the National Nuclear Data Center at Brookhaven National Laboratory.[§]

Advances in buildup factors. Refinements in the computation of buildup factors continued to be made over the years. An adjoint moments method code had come into use (Simmons 1973) and treatment of positron annihilation had been incorporated (Morris et al. 1975). The ASFIT code (Subbaiah et al. 1982; Gopinath et al. 1987), introduced in 1971, and the PALLAS code (Takeuchi et al. 1981, 1984; Tanaka and Takeuchi 1986), introduced in 1973, led ultimately to a comprehensive set of precise buildup factors standardized for use in design and analysis (ANS 1991). The discrete ordinates ASFIT code and the integral-transport PALLAS code account for not only Compton scattering and photoelectric absorption but also positron creation and annihilation, fluorescence, and bremsstrahlung. The evolution of buildup-factor measurements and calculations from 1950 until 1993 was thoroughly documented by Harima (1993).

Working with buildup factors computed using the PALLAS code, Harima developed a data fit in the following form, called the *geometric progression* formula (Harima 1983; Harima et al. 1986, 1991):

$$B(E_o, \mu r) \simeq 1 + (b - 1)(K^{\mu r} - 1)/(K - 1) \tag{13}$$

for $K \neq 1$, and

$$B(E_o, \mu r) \simeq 1 + (b - 1)\mu r$$

for K = 1, where

$$K(\mu r) = c(\mu r)^a + d\frac{\tanh(\mu r/\xi - 2) - \tanh(-2)}{1 - \tanh(-2)},$$

and where *a, b, c, d*, and ξ are parameters that depend on the gamma-ray energy, the attenuating medium, and the nature of the response. This seems to be a very unusual, even bizarre, fitting formula. That may be so, but it is indeed an extraordinarily precise formula, as is illustrated in Fig. 1. Both the results of PALLAS calculations and the coefficients for the geometric progression buildup factors are tabulated in design standards (ANS 1991).

Cross sections and dose conversion factors. Two more foundation stones need to be in place to support a mature radiation shielding technology. One is a comprehensive set of cross sections, or interaction coefficients, accounting for not only reactions but also dosimetry related coefficients such as those for energy deposition. Another is

[§] http://www.nndc.bnl.gov/index.jsp.

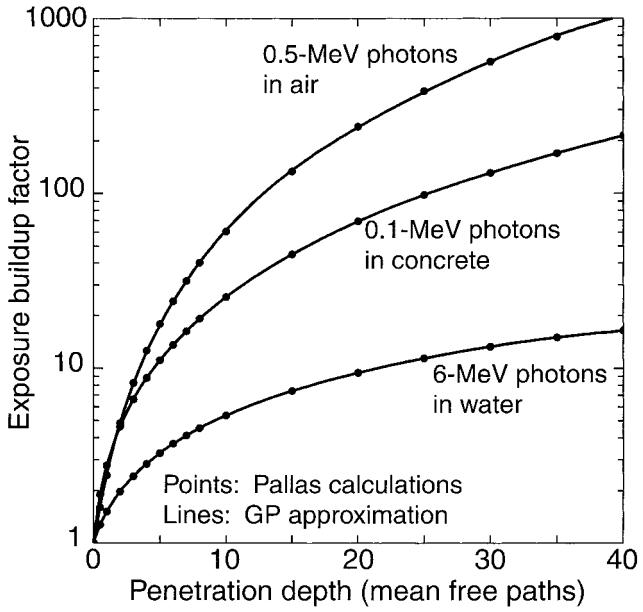

Fig. 1. Comparison of buildup factors computed by the PALLAS code and fit by the geometric progression method.

a set of fluence-to-dose conversion factors applicable to a comprehensive array of dosimetry conditions.

Authoritative cross section data are available in the ENDF/B-6 (evaluated nuclear data file)** database containing evaluated cross sections, spectra, angular distributions, fission product yields, photo-atomic and thermal scattering law data, with emphasis on neutron induced reactions. Data are analyzed and evaluated by experienced nuclear physicists and stored in the internationally adopted format (ENDF-6) maintained by CSEWG, the Cross Section Evaluation Working Group, a cooperative effort of national laboratories, industry, and universities in the United States. ENDF data are processed for use in modern design and analysis computer codes such as MCNP (X-5 2003), DANTSYS (Alcouffe et al. 1995), and TORT (Rhoades and Simpson 1997) and into general purpose packages such as VITAMIN B-6 and BUGLE-96 (White et al. 1995).

The National Institute of Science and Technology (NIST) has long been the repository for gamma-ray interaction coefficients. A sampling of the published data sets may be found in the work of Hubble and Berger (1966), Hubble (1969, 1982), Hubble and Seltzer (1995), and Seltzer (1993). The Institute also sponsors the XCOM cross-section code which may be executed on the NIST internet site†† or downloaded for personal use. Two other sets of photon cross sections (Storm and Israel 1967; Plechaty et al. 1981) have found wide use over the years because they included energy transfer and energy absorption cross sections, essential for fluence-to-dose conversion factors.

Gamma-ray fluence-to-dose conversion factors for local values of exposure or kerma may be computed directly from readily available energy transfer or energy absorption coefficients for air, tissue, etc. Neutron conversion factors for local values of tissue kerma were computed by Caswell et al. (1980). One very important set of conversion factors from the 1970's remains in use. That set is to be used for the deep dose equivalent index‡‡ for neutrons incident on a 30-cm diameter tissue equivalent phantom (NCRP 1971). That set of factors remains in use in the U.S. Nuclear Regulatory Commission regulations for radiation protection, Title 10, Part 20 of the Code of Federal Regulations. As we begin the second century of radiation protection, there are two classes of fluence-to-dose conversion factors in use for neutrons and gamma rays. One very conservative class is to be used for operational purposes at doses well below regulatory limits. This class is based on doses at fixed depths in 30-cm diameter spherical phantoms irradiated in various ways. The other class is to be used for dose assessment purposes, and not for personnel dosimetry. This class is based on the anthropomorphic human phantom and weight factors for effective dose equivalent (ICRP 1987) or effective dose (ICRP 1996).

Computer applications. The 1980's and 1990's were decades of revolution for the computational aspects of radiation shield design and analysis. The advent of inexpensive personal computers with rapidly increasing speeds and memory freed the shielding analyst from dependence on a few supercomputers at national laboratories. Many shielding codes that could previously run only on large mainframe computers were reworked to run on small personal computers thereby allowing any shielding analysts to perform detailed calculations that only a privileged few were able to do previously.

At the same time many improvements were made to the transport codes and their algorithms. MCNP has gone through a series of improvements adding new capabilities and improvements, such as new variance reduction methods, tallies, and physics models. It was translated to the FORTRAN-77 standard in 1983, and to the FORTRAN-90 standard in 2003. New releases appear every few years, and the version as of this writing is MCNP-5. It has also spun off a second version MCNPX with a capability of treating 34 types of particles with energies up to 150 MeV.

General purpose discrete-ordinates codes were extensively improved with many novel acceleration schemes introduced to improve their speeds. An excellent review of many such improvements is given by Adams and Larsen

** http://www.nndc.bnl.gov/exfor/endf00.htm.

†† http://physics.nist.gov/PhysRefData/Xcom/Text/XCOM.html.

‡‡ Maximum dose equivalent at depth of 1 cm or greater.

(2002). Some of the discrete-ordinates codes introduced in these two decades included ONEDANT (O'Dell et al. 1982), TWODANT (Alcouffe et al. 1984), TORT (Rhoades and Childs 1987), DANTSYS (Alcouffe et al. 1995), and PARTISN (Alcouffe et al. 2002).

The future

In many respects, radiation shielding is a mature technological discipline. It is supported by a comprehensive body of literature and a diverse selection of computational resources. The fundamentals and the methodology are readily incorporated into health physics and nuclear engineering education and training programs. It is important that we not allow this maturity to foster complacency. Advances continue to be made in computational resources as well as information on cross sections and material properties, especially radiation resistance. These advances as well as advances in our knowledge of dosimetry and health effects of radiation require continuing attention and adoption into the radiation-shielding discipline. We see this taking place in the efforts of bodies such as the NCRP, ICRP, ICRU, and the BEIR Committees of the National Research Council. We also see it taking place in the maintenance of industrial and manufacturing standards, especially those fostered by the Health Physics Society and the American Nuclear Society.

We close this introduction by reminding readers that there are some important gamma-ray shielding problems that we have not been able to treat using hand calculations or using the design and analysis codes employing point-kernel methods. These include transmission of gamma rays through ducts and passages in structures, reflection of gamma rays from shielding walls and other structures, and transmission of beams of gamma rays obliquely incident on shielding slabs. These problems, like comparable neutron-shielding problems, require full-scale treatment of scattered particles as is done in the Monte Carlo and discrete ordinates computer codes. As computational resources grow, these more advanced transport methods become available on the desks of office, classroom, and home. We expect this trend to continue, and we expect continuing roles for both Monte Carlo and discrete ordinates methods. We take note of efforts at developing hybrid techniques employing both methods and look forward to continued exploitation of these hybrids. We also take note of development of graphical user interfaces to assist users of codes such as the MCNP code. We applaud these efforts and look forward to continuing advances.

PRACTICE OF RADIATION SHIELDING

First it must be said that shielding design and shielding analysis are complementary activities. In design, the source is identified and a target dose goal is specified. The task is to determine the nature of the shielding required to achieve the goal. In analysis, the source and shielding are identified and the task is to determine the consequent dose. Whether one is engaged in a hand calculation or in a most elaborate Monte Carlo simulation, one is faced with the tasks of (1) characterizing the source, (2) characterizing the nature and attenuating properties of the shielding materials, (3) evaluating at a target location the radiation intensity and perhaps its angular and energy distributions, and (4) converting the intensity to a dose or response meaningful in terms of radiation effects.

Basic concepts

Source characterization. Source geometry, energy, and angular distribution are required characteristics. Radionuclide sources, with isotropic emission and unique energies of gamma and x rays are relatively easy to characterize. Activity and source strength must be carefully distinguished, as not every decay results in emission of a particular gamma or x ray. Careful consideration must be given to a low-energy limit below which source particles may be ignored, else computation resources may be wasted. Similarly, when photons of many energies are emitted, as in the case of fission-product sources, one is compelled to use a group structure in source characterization, and much care is needed in establishing efficient and appropriate group energy limits and group average energies. When the source energies are continuously distributed, as is the case with fission neutrons and gamma rays, one option is to use a multi group approach, as might be used in point-kernel calculations. Another option, useful in Monte Carlo simulations, is to sample source energies from a mathematical representation of the energy spectrum.

A point source is very often an appropriate approximation of a physical source of small size. It is also appropriate to represent a line, plane, or volume source as a collection of point sources, as is done in the point-kernel method of shielding analysis. Radionuclide and fission sources are isotropic in angular distribution; however, there are cases for which it is efficient to identify a surface and to characterize the surface as a secondary source surface. Such surface sources are very often non-isotropic in angular distribution. For example, consider the radiation emitted into the atmosphere from a large body of water containing a distributed radiation source. The interface may be treated approximately, but

very effectively, as a plane source emitting radiation not isotropically, but with an intensity varying with the angle of emission from the surface.

Attenuating properties. The total microscopic cross section for an element or nuclide, $\sigma(E)$, multiplied by the atomic density, is the linear interaction coefficient $\mu(E)$, also called the macroscopic cross section, the probability per unit (differential) path length that a particle of energy E interacts with the medium in some way. Its reciprocal, called the *mean free path*, is the average distance traveled before interaction. Usually the ratio μ/ρ, called the mass interaction coefficient, is tabulated because it is independent of density. Various subscripts may be used to designate particular types of interactions, e.g., $\sigma_a(E)$ for absorption or $\sigma_f(E)$ for fission. Likewise, additional independent variables may be introduced, with, e.g., $\sigma_s(E, E')dE'$ representing the cross section for scattering from energy E to an energy between E' and $E' + dE'$. Information resources for attenuating properties are described in this paper's historical review, as are resources for radionuclide decay data.

Intensity characterization. The intensity of a neutron or photon field is ordinarily described in terms of particles crossing the surface of a small spherical volume V. The *fluence* Φ is defined, in the limit $V \to 0$, as the expected or average sum of the path lengths in V traveled by entering particles divided by the volume V. Equivalently, Φ is, again in the limit $V \to 0$, the expected number of particles crossing the surface of V divided by the cross sectional area of the volume. The time derivative of the fluence is the fluence rate or flux density ϕ. Note that the fluence, though having units of reciprocal area, has no reference area or orientation. Note too that the fluence is a point function. The fluence, a function of position, may also be a distribution function for particle energies and directions. For example, $\Phi(\mathbf{r}, E, \mathbf{\Omega})dEd\Omega$ is the fluence at $\mathbf{r}$ of particles with energies in dE about E and with directions in $d\Omega$ about $\mathbf{\Omega}$. When a particular surface is used as a reference, it is useful to define radiation intensity in terms of the flow $J_n(\mathbf{r})$ across the reference surface, as is done in defining the albedo in eqn (11).

Fluence-to-dose conversion factors. Whether the shield designer uses the simplest of the point-kernel methods or the most comprehensive of the Monte Carlo or discrete ordinates methods, fluence-to-dose conversion factors invariably have to be used. The radiation attenuation calculation deals with the particle fluence, the direct measure of radiation intensity. To convert that intensity into a measure of radiation damage or heating of a material, to a field measurement such as exposure, or to a measure of health risk, conversion factors must be applied. Even in that humble health physics thumb rule $6CEN/r^2$ for gamma-ray exposure rate,[§§] the numerical factor incorporates the fluence-to-exposure conversion factor.

The shielding analysis ordinarily yields the energy spectrum $\Phi(\mathbf{r}, E)$ of the photon or neutron fluence at a point identified by the vector $\mathbf{r}$. Use of a Monte Carlo code normally yields the energy spectrum as a continuous function of energy, whence the dose or, more generally, response $D(\mathbf{r})$ is given by the convolution of the fluence with the fluence-to-dose factor, here called the response function $R(E)$, so that

$$D(\mathbf{r}) = \int_E dE R(\mathbf{r}, E)\Phi(\mathbf{r}, E). \tag{14}$$

Point-kernel, or other energy-multigroup methods yield the energy spectrum at discrete energies, or in energy groups, and the dose convolution is a summation rather than an integration.

While the fluence is most always computed as a point function of position, the response of interest may be a dose at a point, or it may be a much more complicated function such as the average radiation dose in a physical volume such as an anthropomorphic phantom. We examine local and phantom-related doses separately. Also, we assume that charged-particle equilibrium*** has been attained, so that the kerma and absorbed dose may be equated.

The local dose. Suppose the local dose of interest is the kerma. Then the response function is given by

$$R(E) = \kappa \sum_i \frac{N_i}{\rho} \sum_j \sigma_{ji}(E)\epsilon_{ji}(E). \tag{15}$$

in which ρ is the mass density, N_i is the atoms of species i per unit volume (proportional to ρ), $\sigma_{ji}(E)$ is the cross section for the jth interaction with species i, and $\epsilon_{ji}(E)$ is the average energy transferred to secondary charged particles in the jth interaction with species i. A units conversion factor κ is needed to convert from, say, units

[§§] The R/h exposure rate at a distance r (ft) in air from C curies of a gamma-ray source emitting, per decay, N gamma rays of energy E (MeV).

*** Under conditions of charged-particle equilibrium, the neutron or gamma ray energy transferred to initial kinetic energy of secondary charged particles is equal to the energy imparted to the medium as manifested in ionization, excitation, chemical change, and heat. Equilibrium is approached in a region of homogeneity in composition and uniformity in neutron or photon intensity.

of MeV cm^{-2} g^{-1} to units of rad cm^{-2} or Gy cm^{-2}. For neutrons, a quality factor multiplier $Q(E)$ is needed to convert to units of dose equivalent (rem or Sv).

Here we need to take note of one very important local-dose response function—the tissue-kerma response function for neutrons. This has been computed by Caswell et al. (1980) for a four-element tissue approximation. Fig. 2 shows the response function based on ENDF/B-V cross sections.

In shielding calculations, one must be very careful to select a response function appropriate to the method used in calculating the fluence energy spectrum $\Phi(\mathbf{r},E)$. Suppose, for example that the photon fluence is computed using an approximation that pair production and the photoelectric effect are purely absorption, i.e., annihilation and fluorescence photons and bremsstrahlung are excluded from Φ. This was a common approximation in the 1940's and 1950's. Then, for the photoelectric and pair production reactions, it is necessary to set $\epsilon_{ji}(E) = E$. Then, in the usual gamma-ray notation, $R(E)$ (Gy cm^{-2}) $= 1.602 \times 10^{-10} E[\mu_a(E)/\rho]$, in which μ_a/ρ is the mass absorption coefficient. On the other hand, if the photon fluence includes Compton-scattered photons, annihilation photons, and fluorescence photons, then the choice is the mass energy transfer coefficient $\mu_{tr}(E)/\rho$. If the photon fluence includes bremsstrahlung as well, then the choice is the mass energy transfer coefficient $\mu_{en}(E)/\rho$. For the special case of gamma or x-ray exposure, the fluence-to-dose conversion factor is given by $R(E)$ (R cm^{-2}) $= 1.835 \times 10^{-8} E[\mu_{en}^{air}(E)/\rho]$.

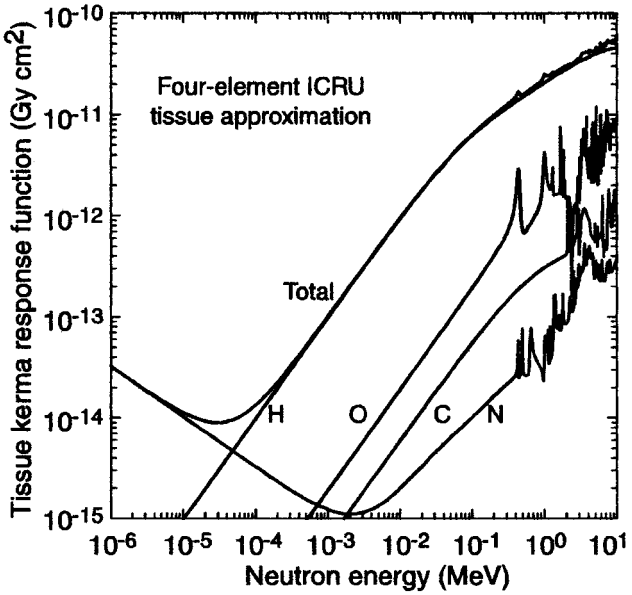

Fig. 2. Kerma response functions for neutron interactions in the ICRU four-element approximation for tissue, with mass fractions 0.101 H, 0.111 C, 0.026 N, 0.762 O. Computed using NJOY-processed ENDF/B-V data.

In point-kernel calculations for gamma rays, it is common practice to first compute the fluence of uncollided photons, then apply a response function to obtain the "uncollided" dose rate, and then a buildup factor to obtain the total dose rate. In these circumstances, it is necessary to apply a response function appropriate to the method used in calculating the buildup factor. If the buildup of secondary photons includes bremsstrahlung as well as annihilation and fluorescence photons, then the appropriate dose conversion factor is based on $\mu_{en}(E)/\rho$.

The phantom-related dose. By phantom-related dose, we mean a local radiation dose within a simple geometric phantom or some sort of average dose within an anthropomorphic phantom. The phantom dose, in fact, is a point function and serves as a standardized reference dose for instrument calibration and radiation protection purposes. Even though the radiation fluence, itself a point function, may have strong spatial and angular variation as well as energy variation, it is still possible to associate with the radiation fluence a phantom-related dose. The procedure is as follows. The fluence is treated, for example, as a very broad parallel beam of the same intensity as the actual radiation field, incident in some fixed way on the phantom. This is the so-called *expanded* and *aligned* field. For a geometric phantom, the dose is computed at a fixed depth. For an anthropomorphic phantom, the dose is computed as an average of doses to particular tissues and organs, weighted by the susceptibility of the tissues and organs to radiation carcinogenesis or hereditary illness.

Geometric phantoms are used for operational radiation-protection applications, i.e., at doses well below regulatory limits. Slabs, cylinders, and spheres have all been used as geometric phantoms, but the 30-cm-diameter "ICRU Sphere" has become the standard.[†††] This is a sphere of density 1 g cm^{-3} comprised of a four-element tissue approximation, 76.2% by weight oxygen, 11.1% carbon, 10.1% hydrogen, and 2.6% nitrogen. Fluence-to-dose conversion factors are available for four irradiation geometries: (PAR), a single plane parallel beam; this is the default geometry suitable for instrument calibration; (OPP), two opposed plane parallel beams; (ROT), a rotating plane parallel beam (i.e., a plane parallel beam with the sphere rotating about an axis normal to the beam); and (ISO), an isotropic radiation field. Fluence-to-dose conversion factors are tabulated in

[†††] An exception is the use of a 30-cm cylindrical phantom for the neutron fluence-to-dose conversion factors listed in the regulations of the U.S. Nuclear Regulatory Commission, as recommended by the NCRP (1971). Furthermore, the dose computed is not the 10-mm ambient dose, but rather the deep dose equivalent index, the maximum dose at a depth of 10 mm or greater in the phantom.

reports of the ICRP (1987, 1996) and reproduced by Shultis and Faw (2000).

Dose conversion factors are also available for three depths of penetration into the geometric phantom: (1) A 10-mm depth, the dose being called the *ambient dose*, a surrogate to the earlier *whole body dose* and the dose suitable for instrument calibration; (2) a 3-mm depth, suitable for representing the dose to the lens of the eye; and (3) a 0.07-mm depth, suitable for representing the dose to the skin.

Anthropomorphic phantoms are mathematical descriptions of the organs and tissues of the human body, formulated in such a way as to permit calculation or numerical simulation of the transport of radiation throughout the body. In calculations leading to response functions, monoenergetic radiation is incident on the phantom in fixed geometry. One geometry leading to conservative values of response functions is anteroposterior (AP), irradiation from the front to the back with the beam at right angles to the long axis of the body. Other geometries are posteroanterior (PA), right and left lateral (RLAT and LLAT), rotational (ROT), and isotropic (ISO). The AP case, being most conservative, is the choice in the absence of particular information on the irradiation circumstances.

Figs. 3 and 4 compare response functions for photons and neutrons, respectively. At energies above about 0.1 MeV, the various photon response functions are very nearly equal. This is a fortunate situation for radiation dosimetry and surveillance purposes. Personnel dosimeters are usually calibrated to give responses proportional

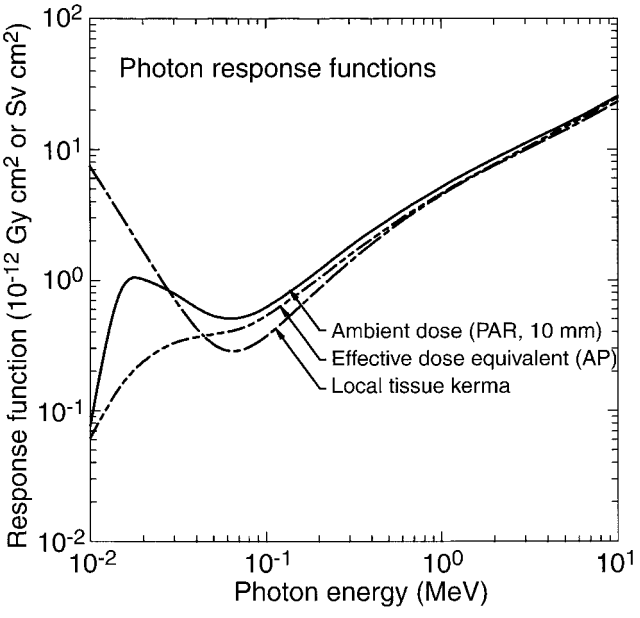

Fig. 3. Comparison of photon response functions. Data are from ICRP (1987).

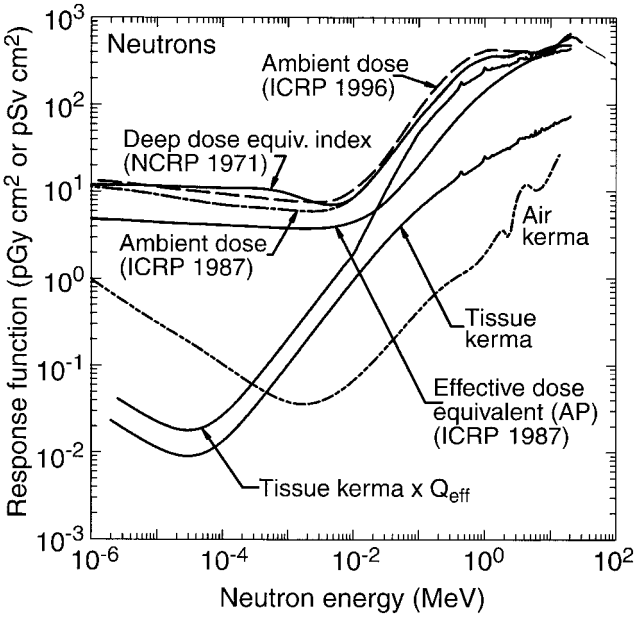

Fig. 4. Various neutron response functions.

to the ambient dose. Both the ambient dose and the tissue kerma closely approximate the effective dose equivalent.

The comparison of response functions for neutrons is not so straightforward. The tissue kerma always has the smallest response function, largely because no quality factor is applied to the kinetic energy of a secondary charged particle. Furthermore, the ambient dose always exceeds the effective dose equivalent. Thus, calibration of personnel dosimeters in terms of ambient dose is a conservative practice.

Basic analysis methods

In this section fundamental methods for estimating neutron or photon doses are reviewed. Such indirectly ionizing radiation is characterized by straight-line trajectories punctuated by "point" interactions. The basic concepts presented here apply equally to all particles of such radiation.

It should be noted that throughout this paper, calculated doses are the expected or average value of the stochastic measured doses, i.e., the mechanistically calculated dose represents the statistical average of a large number of dose measurements which exhibit random fluctuations as a consequence of the stochastic nature of the source emission and interactions in the detector and surrounding material.

Uncollided radiation doses. In many situations the dose at some point of interest is dominated by particles streaming directly from the source without interacting in the surrounding medium. For example, if only air separates a gamma-ray or neutron source from a detector,

interactions in the intervening air or in nearby solid objects, such as the ground or building walls, are often negligible, and the radiation field at the detector is due almost entirely to uncollided radiation coming directly from the source.

In an attenuating medium, the uncollided dose at a distance r from a point isotropic source emitting S_p particles of energy E is

$$D^o(r) = \frac{S_p R}{4\pi r^2} e^{-\ell} \tag{16}$$

where ℓ is the total number of mean-free-path lengths of material a particle must traverse before reaching the detector, namely, $\int_0^r ds\ \mu(s)$. Here R is the appropriate response function. The $1/(4\pi r^2)$ term in eqn (16) is often referred to as the geometric attenuation and the $e^{-\ell}$ term the material attenuation. Eqn (16) can be extended easily to a source emitting particles with different discrete energies or a continuous spectrum of energies.

Point kernel for uncollided dose. Consider an isotropic point source placed at $\mathbf{r}_s$ and an isotropic point detector (or target) placed at $\mathbf{r}_t$ in an homogeneous medium. The detector response depends not on $\mathbf{r}_s$ and $\mathbf{r}_t$ separately, but only on the distance $|\mathbf{r}_s - \mathbf{r}_t|$ between the source and detector. For a unit strength source the detector response is (cf. eqn 16):

$$G^o(\mathbf{r}_s, \mathbf{r}_t, E) = \frac{R(E)}{4\pi|\mathbf{r}_s - \mathbf{r}_t|^2} e^{-\mu(E)|\mathbf{r}_s - \mathbf{r}_t|}. \tag{17}$$

Here $G^o(\mathbf{r}_s, \mathbf{r}_t, E)$ is the *uncollided dose point kernel* and equals the dose at $\mathbf{r}_t$ per particle of energy E emitted isotropically at $\mathbf{r}_s$. This result holds for any geometry or medium provided that the material through which a ray from $\mathbf{r}_s$ to $\mathbf{r}_t$ passes has a constant interaction coefficient μ.

With this point kernel, the uncollided dose due to an arbitrarily distributed source can be found by first decomposing (conceptually) the source into a set of contiguous effective point sources and then summing (integrating) the dose produced by each point source.

Applications to selected geometries. The results for the uncollided dose from a point source can be used to derive expressions for the uncollided dose arising from a wide variety of distributed sources such as line sources, area sources, and volumetric sources (Rockwell 1956; Blizard and Abbott 1962; Jaeger 1968; Schaeffer 1973). An example to illustrate the method is as follows.

A straight-line source of length L emitting isotropically S_l particles per unit length at energy E is depicted in Fig. 5. A detector is positioned at point P, a distance h from the source along a perpendicular to one end of the line. Suppose the only material separating the line source and the receptor is a slab of thickness t and total attenuation coefficient μ_s.

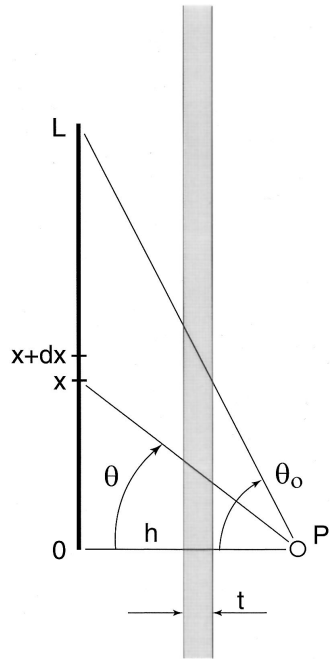

Fig. 5. Isotropic line source with a slab shield.

Consider a segment of the line source between distance x and $x + dx$ measured from the bottom of the source. The source within this segment may be treated as an effective point isotropic source emitting $S_l\ dx$ particles, which produces an uncollided dose at P of dD^o. The ray from the source in dx must pass through a slant distance of the shield t sec θ so that the dose at P from particles emitted in dx about x is

$$dD^o(P) = \frac{1}{4\pi} \frac{S_l R\ dx}{x^2 + h^2} \exp[-\mu t \sec\theta], \tag{18}$$

where R and μ generally depend on the particle energy E. To obtain the total dose at P from all segments of the line source, one then must sum, or rather integrate, dD^o over all line segments. As can be seen from Fig. 5, $x = h \tan\theta$ and $x^2 + h^2 = h^2 \sec^2\theta$. It then follows that $dx = h \sec^2\theta\, d\theta$, so that the total uncollided dose at P becomes

$$D^o(P) = \frac{S_l R}{4\pi h} \int_0^{\theta_o} d\theta e^{-\mu t \sec\theta} = \frac{S_l R}{4\pi h} F(\theta_o, \mu_s t), \tag{19}$$

where the *Sievert integral* or the *secant integral* F is defined as $F(\theta, b) \equiv \int_0^\theta dy\ e^{-b \sec y}$.

Intermediate methods for photon shielding

In this section we summarize several special techniques for the design and analysis of shielding for

gamma and x rays with energies from about 1 keV to about 20 MeV. These techniques are founded on very precise radiation transport calculations for a wide range of carefully prescribed situations. These techniques, which rely on buildup factors, attenuation factors, albedos or reflection factors, and line-beam response functions, then allow estimation of photon doses for many common shielding situations without the need of transport calculations.

Buildup factor concept. The total photon fluence $\Phi(\mathbf{r}, E)$ at some point of interest $\mathbf{r}$ is the sum of two components: the uncollided fluence $\Phi^o(\mathbf{r}, E)$ of photons that have streamed to $\mathbf{r}$ directly from the source without interaction, and the scattered or secondary photon fluence $\Phi^s(\mathbf{r}, E)$ consisting of source photons scattered one or more times, as well as secondary photons such as x rays and annihilation gamma rays.

The buildup factor $B(\mathbf{r})$ is defined in eqn (6) and, for monoenergetic sources, in eqn (7). By far the largest body of buildup-factor data is for point, isotropic, and monoenergetic sources of photons in infinite homogeneous media. Calculation of buildup factors for high-energy photons requires consideration of the paths traveled by positrons from their creation until their annihilation. Such calculations have been performed by Hirayama (1987) and by Faw and Shultis (1993) for photon energies as great as 100 MeV. Because incoherent scattering was neglected in many buildup factor calculations, coherent scattering should also be neglected in calculating the uncollided dose, a significant consideration only for low energy photons at deep penetration.

Buildup factor geometry. Buildup factors generally depend on the source and shield geometries. For the same material thickness between source and detector, buildup factors are slightly different for point isotropic sources in (a) an infinite medium, (b) at the surface of a bare sphere, and for a slab shield between source and detector. However, the use of buildup factors for a point isotropic source is almost always conservative, i.e., the estimated dose is greater than that for a finite shield (Shultis and Faw 2000). Adjustment factors for buildup factors at the surface of a finite medium in terms of the infinite medium buildup factors are illustrated in Fig. 6.

Buildup factors are also available for plane isotopic (PLI) and plane monodirectional (PLM) gamma-ray sources in infinite media. Indeed, Fano et al. (1959), Goldstein (1959), and Spencer (1962), in their moments-method calculations, obtained buildup factors for plane sources first and, from these, buildup factors for point sources. Buildup factors at depth in a half-space shield are also available for the PLM source, that is, normally

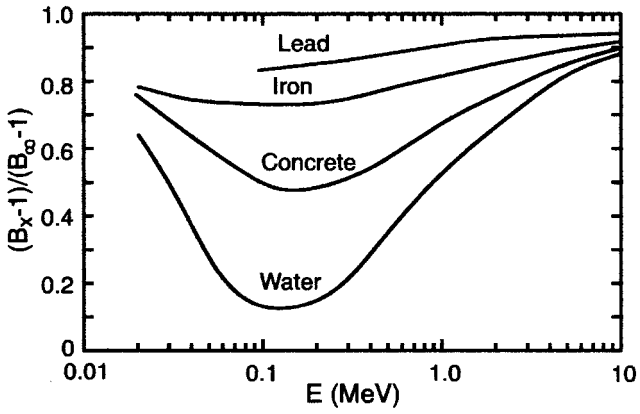

Fig. 6. Adjustment factors for the buildup factor B_x at the boundary of a finite medium in terms of the infinite-medium buildup factor B_∞ for the same depth of penetration. EGS4 calculations courtesy of Sherrill Shue, Nuclear Engineering Department, Kansas State University.

incident photons (Takeuchi et al. 1981; Takeuchi and Tanaka 1984; Hirayama 1987). Again, the use of buildup factors for a point isotropic source in an infinite medium for these geometries is conservative.

Buildup in stratified media. The use of the buildup-factor concept for heterogeneous media is of dubious merit for the most part. Nevertheless, implementation of point-kernel codes for shielding design and analysis demands some way of treating buildup when the path from source point to dose point is through more than one shielding material. Certain regularities do exist, however, which permit at least approximate use of homogeneous-medium buildup factors for stratified shields. Many approximate methods have been suggested, as described by Shultis and Faw (2000); however, they are of little use in point-kernel calculations and of no need in transport methods of shielding analysis.

Point-kernel computer codes. There are many codes in wide use that are based on the point-kernel technique. In these codes a distributed source is decomposed into small but finite elements and the dose at some receptor point from each element is computed using the uncollided dose kernel and a buildup factor based on the optical thickness of material between the source element and the receptor. The results for all the source elements are then added together to obtain the total dose. Some that have been widely used are MicroShield (Negin and Worku 1998), the QAD series [QAD (Malenfant 1967), QAD-CG (Cain 1977), QADMOD (Price and Blattner 1979)], and G^3 (Malenfant 1973).

Broad-beam attenuation. Often a point radionuclide or x-ray source in air is located sufficiently far from

a wall or shielding slab that the radiation reaches the wall in nearly parallel rays. Further, the attenuation in the air is quite negligible in comparison to that provided by the shielding wall. Shielding design and analysis for such broad-beam illumination of a slab shield are addressed by NCRP Report 49 (1976), Archer (1995), and Simpkin (1989). The dose at the surface of the cold side of the wall can be computed as

$$D = D^o A_f. \tag{20}$$

For a radionuclide source of activity C, the dose D^o without the wall can be expressed in terms of the source energy spectrum, response functions, and distance r from the source to the cold side of the wall. Then

$$D = D^o A_f = \frac{C}{r^2}\Gamma A_f, \tag{21}$$

where Γ is a *specific gamma-ray constant*, that is, the dose rate in vacuum at a unit distance from a source with unit activity, and A_f is an *attenuation factor* which depends on the nature and thickness of the shielding material, the source energy characteristics, and the angle of incidence ϑ (with respect to the wall normal). Values for Γ and A_f are provided by NCRP (1976).

Oblique incidence. Attenuation factors for obliquely incident beams are presented in NCRP Report 49 (1976). For such cases, special three-argument slant-incidence buildup factors should be used (Shultis and Faw 2000). For a shield wall of thickness t mean free paths, slant incidence at angle ϑ with respect to the normal to the wall, and source energy E_o, the attenuation factor is in function form $A_f(E_o, t, \vartheta)$. However, a common, but erroneous, practice has been to use a two-argument attenuation factor based on an infinite medium buildup factor for slant penetration distance t sec ϑ, in the form $A_f(E_o, t \sec \vartheta)$. This practice can lead to severe under prediction of radiation dose.

X-ray beam attenuation. For x-ray sources, the appropriate measure of source strength is the electron-beam current i, and the appropriate characterization of photon energies, in principle, involves the peak accelerating voltage (kVp), the wave form, and the degree of filtration (e.g., beam half-value thickness). If i is the beam current (mA) and r is the source-detector distance (m), the dose behind a broadly illuminated shield wall is

$$D(P) = \frac{i}{r^2}K_o A_f, \tag{22}$$

in which K_o is the *radiation output (factor)*, the dose rate in vacuum (or air) per unit beam current at unit distance from the source in the absence of the shield. Empirical formulas for computing A_f are available for shield design (Archer et al. 1983, 1994; Simpkin 1995).

Intermediate methods for neutron shielding

Shielding design for fast neutrons is far more complex than shielding design for photons. Besides having to protect against the neutrons emitted by some source, there are primary gamma rays produced by most neutron sources, and secondary photons produced by inelastic neutron scattering and from radiative capture. There may also be secondary neutrons produced from $(n,2n)$ and fission reactions. In many instances, secondary photons produce greater radiological risks than do the primary neutrons. Fast-neutron sources include spontaneous and induced fission, fusion, (α, n) reactions, (γ, n) reactions, and spallation reactions in accelerators, each producing neutrons with a different distribution of energies.

Unlike photon cross sections, neutron cross sections usually vary greatly with neutron energy and among the different isotopes of the same element. Large cross-section data bases are needed. Also, because of the erratic variation of the cross sections with energy, it is difficult to calculate uncollided doses needed in order to use the buildup factor approach. Moreover, buildup factors are very geometry dependent and sensitive to the energy spectrum of the neutron fluence and, consequently, point-kernel methods can be applied to neutron shielding only in very limited circumstances.

Early work led to kernels for fission sources in aqueous systems, as described by eqns (3) and (4), and to the use of removal cross sections, eqn (5), to account for shielding barriers. Over the years, the methodology was stretched to apply to non-aqueous hydrogenous media, then to non-hydrogenous media, then to sources other than fission. Elements of diffusion and age theory were melded with the point kernels. Today, with the availability of massive computer resources, neutron shielding design and analysis is largely done using transport methods. Nevertheless, the earlier methodology offers insight allowing more critical interpretation of results of transport calculations.

Also, unlike ratios of different photon response functions, those for neutrons vary, often strongly, with neutron energy (see Fig. 4). Hence neutrons doses cannot be converted to different dose units by simply multiplying by an appropriate constant. The energy spectrum of the neutron fluence is needed to obtain doses in different units. Consequently, many old measurements or calculations of point kernels, albedo functions, transmission factors, etc., made with obsolete dose units cannot be converted to modern units because the energy spectrum

is unknown or lost. In this case there is no recourse but to repeat the measurements or calculations.

Capture-gamma photons. A significant, often dominant, component of the total dose at the surface of a shield accrues from capture gamma photons produced deep within the shield arising from neutron absorption. Of lesser significance are secondary photons produced in the inelastic scattering of fast neutrons. Secondary neutrons are also produced as a result of (γ, n) reactions. Thus, in transport methods, gamma-ray and neutron transport are almost always coupled.

Historically, capture gamma-ray analysis was appended to neutron removal calculations. Most neutrons are absorbed only when they reach thermal energies, and, consequently, only the absorption of thermal neutrons was considered.[‡‡‡] For this reason it is important to calculate accurately the thermal neutron fluence $\Phi_{th}(\mathbf{r})$ in the shield. The volumetric source strength of capture photons per unit energy about E is then given by

$$S_\gamma(\mathbf{r}, E) = \Phi_{th}(\mathbf{r})\mu_\gamma(\mathbf{r})\, f(\mathbf{r}, E), \qquad (23)$$

where $\mu_\gamma(\mathbf{r})$ is the absorption coefficient at $\mathbf{r}$ for thermal neutrons and $f(\mathbf{r}, E)$ is the number of photons produced in unit energy about E per thermal neutron absorption at $\mathbf{r}$.

Once the capture-gamma ray source term $S_\gamma(\mathbf{r},E)$ is known throughout the shield, point-kernel techniques using exponential attenuation and buildup factors can be used to calculate the gamma-ray dose at the shield surface.

Neutron shielding with concrete. Concrete is probably the most widely used shielding material because of its relatively low cost and the ease with which it can be cast into large and variously shaped shields. However, unlike that for photon attenuation in concrete, the concrete composition, especially the water content, has a strong influence on its neutron attenuation properties. Other important factors that influence the effectiveness of concrete as a neutron shield include type of aggregate, the dose response function, and the angle of incidence of the neutrons.

Because concrete is so widely used as a shield material, its effectiveness for a monoenergetic, broad, parallel beam of incident neutrons has been extensively studied, both for normal and slant incidence, and many tabulated results for shields of various thickness are available (Chilton 1969, 1971; Roussin and Schmidt 1971; Roussin et al. 1973; Wyckoff and Chilton 1973; Wang and Faw 1995). These tabulated results are extremely useful in the preliminary design of concrete shields.

[‡‡‡] Exceptional cases include the strong absorption of epithermal neutrons in fast reactor cores or in thick slabs of low-moderating, high-absorbing material.

Gamma-ray and neutron reflection

So far in this discussion, we have dealt with shielding situations in which, for radiation reaching a target, there is a component of uncollided radiation. Then, in principle, point-kernel approximations may be used and concepts such as particle buildup may be applied. In many problems of shielding design and analysis, only scattered radiation may reach a target. Radiation dose due to reflection from a surface is an example that arises in treatment of streaming of radiation through multilegged ducts and passageways. Treatment of radiation reflection from structure surfaces is also a necessary adjunct to precise calibration of nuclear instrumentation. Skyshine, i.e., reflection in the atmosphere of radiation from fixed sources to distant points, is another example of this class of problem. All such reflection problems are impossible to treat using elementary point-kernel methods and very difficult and inefficient to treat using transport methods. For reflection from a surface of radiation from a point source to a point receiver, the *albedo function* has come to be very useful in design and analysis. The same can be said for use of the *line beam response function* in treatment of skyshine.

Albedo methods. There are frequent instances for which the dose at some location from radiation reflected from walls and floors may be comparable to the line-of-sight dose. The term *reflection* in this context does not imply a surface scattering. Rather, gamma rays or neutrons penetrate the surface of a shielding or structural material, scatter within the material, and then emerge from the material with reduced energy and at some location other than the point of entry.

In many such analyses, a simplified method, called the *albedo method*, may be used. The albedo method is based on the following approximations: (1) the displacement between points of entry and emergence may be neglected; (2) the reflecting medium is effectively a half-space, a conservative approximation; (3) scattering in air between a source and the reflecting surface and between the reflecting surface and the detector may be neglected.

Application of the albedo method. Radiation reflection may be described in terms of the geometry shown in Fig. 7 and eqns (11) and (12). Suppose that a point isotropic and monoenergetic source is located distance r_1 from area dA along incident direction $\mathbf{\Omega}_o$ and that a dose point is located distance r_2 from area dA along

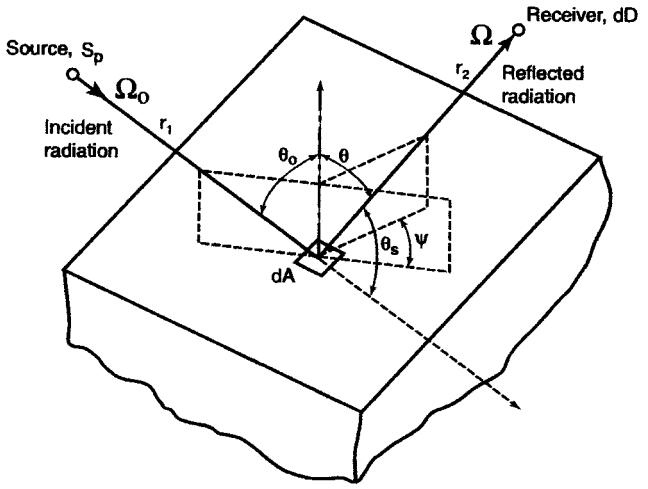

Fig. 7. Angular and energy relationships in the albedo formulation.

emergent direction $\mathbf{\Omega}$. Suppose also the source has an angular distribution such that $S(\vartheta_o)$ is the source intensity per steradian, evaluated at the direction from the source to the reflecting area dA. Then the dose dD_r at the detector from particles reflected from dA can be shown to be (Shultis and Faw 2000)

$$dD_r = D_o \alpha_D(E_o,\ \vartheta_o;\ \vartheta,\ \psi)\frac{dA\ \cos\ \vartheta_o}{r_2^2}, \qquad (24)$$

in which D_o is the dose at dA due to incident particles. Determination of the total reflected dose D_r requires integration over the area of the reflecting surface. Doing so must acknowledge that as the location on the surface changes, all the variables ϑ_o, ϑ, ψ, r_1, and r_2 change as well. Also, it is necessary to know $\alpha_D(E_o,\vartheta_o;\ \vartheta,\psi)$ or, more usefully, to have some analytical approximation for the dose albedo so that integration over all areas can be performed efficiently.

Gamma-ray dose albedo approximations

A two-parameter approximation for the photon dose albedo was first devised by Chilton and Huddleston (1963) and later extended by Chilton et al. (1965). Chilton (1967) later proposed a more accurate 7-parameter albedo formula for concrete. Brockhoff (2003) published seven-parameter fit data for albedos from water, concrete, iron, and lead. Two examples of this dose albedo approximation are shown in Fig. 8.

Neutron dose albedo approximations. The dose albedo concept is very useful for streaming problems that involve "reflection" of neutrons or photons from some material interface. However, unlike photon albedos, the neutron albedos are seldom tabulated or approximated for monoenergetic incident neutrons because of the rapid

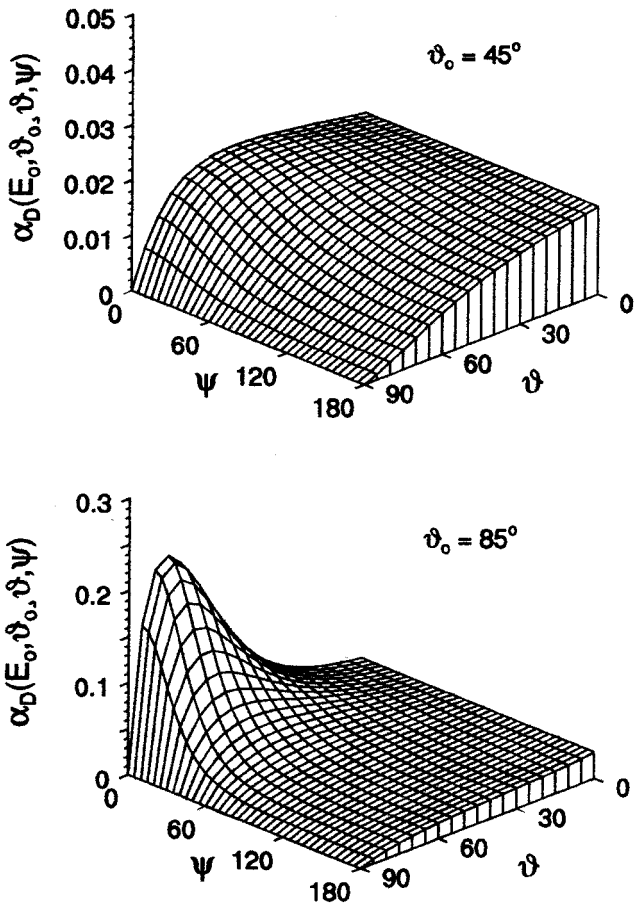

Fig. 8. Ambient-dose-equivalent albedos for reflection of 1.25-MeV photons from concrete, computed using the seven-term Chilton-Huddleston approximation.

variation with energy of neutron cross sections. Rather, albedos for neutrons with a specific range of energies (energy group) are usually considered, thereby averaging over all the cross section resonances in the group. Also unlike photon albedos, neutron albedos involve reflected dose from both neutrons and secondary capture gamma rays.

There are many studies of the neutron albedos in the literature. Selph (1973) published a detailed review. Extensive compilations of neutron albedo data are available, for example, SAIL (Simmons et al. 1979) and BREESE-II (Cain and Emmett 1979). Of more utility are analytic approximations for the albedo based on measured or calculated albedos. Neutrons albedos are often divided into three types: (1) fast neutron albedos ($E \geq 0.2$ MeV), (2) intermediate energy albedos, and (3) thermal-neutron albedos. Selph (1973) reviews early approximations for neutron albedos, among which is a 24-parameter approximation developed by Maerker and Muckenthaler (1965).

Newly computed fast-neutron albedos, also in a 24-parameter approximation, were computed by Brockhoff (2003).

For neutrons with energy less than about 100 keV, the various dose equivalent response functions are very insensitive to neutron energy. Consequently, the dose albedo α_D is very closely approximated by the number albedo α_N. Thus, for reflected dose calculations involving intermediate or thermal neutrons, the number albedo is almost always used. Coleman et al. (1967) calculated neutron albedos for intermediate-energy neutrons (200 keV to 0.5 eV) incident monodirectionally on reinforced concrete slabs and developed a 9-parameter formula for the albedo.

Thermal neutrons entering a shield undergo isotropic scattering that, on the average, does not change their energies. For one-speed particles incident in an azimuthally symmetric fashion on a half-space of material that isotropically scatters particles, Chandrasekhar (1960) derived an exact expression for the differential albedo. A purely empirical and particularly simple formula, based on Monte Carlo data for thermal neutrons, has been proposed by Wells (1964) for ordinary concrete, namely,

$$\alpha_N(\vartheta_o;\ \vartheta,\ \psi) = 0.21\ \cos\vartheta(\cos\vartheta_o)^{-1/3}. \quad (25)$$

Radiation streaming through ducts. Except in the simplest cases, the analysis of radiation streaming requires advanced computational procedures. However, even within the framework of Monte Carlo transport calculations, albedo methods are commonly used, and special data sets have been developed for such use (Simmons et al 1979; Cain and Emmett 1979; Gomes and Stevens 1991).

Elementary methods for gamma-ray streaming are limited to straight cylindrical ducts, with incident radiation symmetric about the duct axis and uniform over the duct entrance. Transmitted radiation generally may be subdivided into three components: line-of-sight, lip-penetrated, and wall scattered. The first two may be treated using point-kernel methodology. The last requires use of albedo methods to account for scattering over the entire surface area of the duct walls. Selph (1973) reviews the methodology of duct transmission calculations and LeDoux and Chilton (1959) devised a method of treating two-legged rectangular ducts, which is important in analysis of structure shielding.

Neutron streaming through gaps and ducts in a shield is much more serious for neutrons than for gamma photons. Neutron albedos, especially for thermal neutrons, are generally much higher than those for photons, and multiple scattering within the duct is very important. Placing bends in a duct, which is very effective for reducing gamma-ray penetration, is far less effective for neutrons. Fast neutrons entering a duct in a concrete shield become thermalized and thereafter are capable of scattering many times, allowing the neutrons to stream through the duct, even those with several bends. Also, unlike gamma-ray streaming, the duct need not be a void (or gas filled) but can be any part of a heterogeneous shield that is "transparent" to neutrons. For example, the steel walls of a water pipe embedded in a concrete shield (such as the cooling pipes that penetrate the biological shield of a nuclear reactor) act as an annular duct for fast neutrons.

There is much literature on experimental and calculational studies of gamma-ray and neutron streaming through ducts. In many of these studies empirical formulas, obtained by fits to the data, have been proposed. These formulas are often useful for estimating duct-transmitted doses under similar circumstances. As a starting point for finding such information, the interested reader is referred to Rockwell (1956), Selph (1973), and NCRP (2003).

Gamma-ray and neutron skyshine. For many intense localized sources of radiation, the shielding against radiation that is directed skyward is usually far less than that for the radiation emitted laterally. However, the radiation emitted vertically into the air undergoes scattering interactions and some radiation is reflected back to the ground, often at distances far from the original source. This atmospherically reflected radiation, referred to as skyshine, is of concern both to workers at a facility and to the general population outside the facility site.

As alternatives to rigorous transport-theory treatment of the skyshine problem, several approximate procedures have been developed for both gamma-photon and neutron skyshine sources (Shultis et al. 1991). This section summarizes one approximate method, which has been found useful for bare or shielded skyshine sources. The *integral line-beam skyshine method* is based on the availability of a line-beam response function $R(E, \varphi, x)$, which gives the dose (air kerma or ambient dose) at a distance x from a point source emitting a photon or neutron of energy E at an angle φ from the source-to-detector axis into an infinite air medium. The air-ground interface is neglected in this method. This response function can be fit over a large range of x to the following three-parameter empirical formula, for a fixed value of E and φ (Lampley et al. 1988):

$$R(E, \varphi, x) = \kappa(\rho/\rho_o)^2 E[x(\rho/\rho_o)]^b \exp[a - cx(\rho/\rho_o)], \quad (26)$$

in which ρ is the air density in the same units as the reference density $\rho_o = 0.0012$ g cm^{-3}. The constant κ depends on the choice of units.

The parameters a, b, and c in eqn (26) depend on the photon or neutron energy and the source emission angle. These parameters have been estimated and tabulated for fixed values of E and φ by fitting eqn (26) to values of the line-beam response function, at different x distances, usually obtained by Monte Carlo calculations. Gamma-ray response functions have been published by Lampley (1979) and Brockhoff et al. (1996). Neutron and secondary gamma-ray response functions have been published by Lampley (1979) and Gui et al. (1997). These data and their method of application are presented by Shultis and Faw (2000).

To obtain the skyshine dose $D(d)$ at a distance d from a bare collimated source, the line-beam response function, weighted by the energy and angular distribution of the source, is integrated over all source energies and emission directions. Thus, if the collimated source emits $S(E, \mathbf{\Omega})$ photons, the skyshine dose is

$$D(d) = \int_0^\infty dE \int_{\Omega_s} d\Omega S(E, \mathbf{\Omega}) R(E, \varphi, d), \quad (27)$$

where the angular integration is over all emission directions $\mathbf{\Omega}_s$ allowed by the source collimation. Here φ is a function of thee mission direction $\mathbf{\Omega}$. To obtain this result, it has been assumed that the presence of an air-ground interface can be neglected by replacing the ground by an infinite air medium. The effect of the ground interface on the skyshine radiation, except at positions very near a broadly collimated source, has been found to be very small.

The presence of a shield over a skyshine source, for example, a building roof, causes some of the source particles penetrating the shield to be degraded in energy and angularly redirected before being transported through the atmosphere. The effect of an overhead shield on the skyshine dose far from the source can be accurately treated by a two-step hybrid method (Shultis et al. 1991; Stedry 1994). First a transport calculation is performed to determine the energy and angular distribution of the radiation penetrating the shield, and then, with this distribution as an effective point, bare skyshine source, the integral line-beam method is used to evaluate the skyshine dose.

The integral line-beam method for gamma-ray and neutron skyshine calculations has been applied to a variety of source configurations and found to give generally excellent agreement with benchmark calculations and experimental results (Shultis et al. 1991). It has been used as the basis of the microcomputer code *MicroSkyshine* (Negin 1987) for gamma rays. A code package for both neutron and gamma-ray calculations is available from the Radiation Safety Computation Information Center.[§§§]

Transport theory

For difficult shielding problems in which simplified techniques such as point kernels with buildup corrections cannot be used, calculations based on transport theory must often be used. There are two basic approaches for transport calculations: *deterministic* transport calculations in which the linear Boltzmann equation is solved numerically, and *Monte Carlo* calculations in which a simulation is made of how particles migrate stochastically through the problem geometry. Both approaches have their advantages and weaknesses. Because of space limitations, we are unable to give a detailed review of the vast literature supporting both approaches. Below a brief explanation of the basic ideas involved and some general references are presented.

Deterministic transport theory. The neutron or photon flux $\phi(\mathbf{r}, E, \mathbf{\Omega})$ for particles with energy E and direction $\mathbf{\Omega}$ is rigorously given by the linear Boltzmann equation or, simply, the transport equation

$$\mathbf{\Omega} \cdot \nabla \phi(\mathbf{r}, E, \mathbf{\Omega}) + \mu(\mathbf{r}, E)\phi(\mathbf{r}, E, \mathbf{\Omega}) = S(\mathbf{r}, E, \mathbf{\Omega}) + \int_0^\infty dE' \int_{4\pi} d\Omega' \, \mu_s(\mathbf{r}, E', \mathbf{\Omega}' \rightarrow E, \mathbf{\Omega}) \phi(\mathbf{r}, E', \mathbf{\Omega}'), \quad (28)$$

where S is the volumetric source strength of particles. This equation can be formally integrated to yield the integral form of the transport equation, namely,

$$\phi(\mathbf{r}, E, \mathbf{\Omega}) = \phi(\mathbf{r} - R\mathbf{\Omega}, E, \mathbf{\Omega}) f(R) + \int_0^R dR' \, q(\mathbf{r} - R'\mathbf{\Omega}, \mathbf{\Omega}) f(R'), \quad (29)$$

$$\text{where } f(x) \equiv \exp\left[-\int_0^x \mu(\mathbf{r} - R''\mathbf{\Omega}, E) dR''\right]$$

and q is given by

[§§§] Code package CCC-646: SKYSHINE-KSU: Code System to Calculate Neutron and Gamma-Ray Skyshine Doses Using the Integral Line-Beam Method, and data library DLC-188: SKYDATA-KSU: Parameters for Approximate Neutron and Gamma-Ray Skyshine Response Functions and Ground Correction Factors.

$$q(\mathbf{r}, E, \mathbf{\Omega}) \equiv S(\mathbf{r}, E, \mathbf{\Omega}) + \int_0^\infty dE' \int_{4\pi} d\Omega'\, \mu_s(\mathbf{r}, E', \mathbf{\Omega}' \rightarrow E, \mathbf{\Omega}) \phi(\mathbf{r}, E', \mathbf{\Omega}'). \quad (30)$$

Unfortunately, neither of these formulations of the transport equation can be solved analytically except for idealistic cases, e.g., infinite medium with monoenergetic particles. Numerical solutions must be used for all practical shielding analyses. Many approximations of the transport equation are used, such as diffusion theory, to allow easier calculations. The energy multigroup approximation is almost always used in which the group averaged cross sections depend on an assumed energy spectrum of the radiation. Even with an energy multigroup approximation, numerical solutions are still computationally formidable.

The most widely used deterministic transport approach is the discrete-ordinates method. In this method a spatial and directional mesh is created for the problem geometry, and the multigroup form of the transport equation is then integrated over each spatial and directional cell. The solution of the approximating algebraic equations is then accomplished by introducing another approximation that relates the cell-centered flux densities to those on the cell boundaries, and an iterative procedure between the source (scattered particles and true source particles) and flux density calculation is then used to calculate the fluxes at the mesh nodes. For details of this method the reader is referred to Carlson and Lathrop (1968), Duderstadt and Martin (1979), and Lewis and Miller (1984).

Discrete ordinates calculations can be computationally expensive because of the usually enormous number of mesh nodes and the fact that the convergence of an iterative solution is often very slow. A subject of great interest in the last thirty years has been the development of numerous methods to accelerate convergence of the iterations. Without convergence acceleration schemes, discrete ordinate solutions would be computationally impractical for many shielding problems. An excellent description of the various acceleration schemes that have been used is provided by Adams and Larsen (2002).

Mature computer codes based on the discrete-ordinates method are widely available to treat one-, two-, and three-dimensional problems in the three basic geometries (rectangular, spherical, and cylindrical) with an arbitrary number of energy groups (Rhoades and Childs 1987; Alcouffe et al. 2002).

Although discrete-ordinates methods are widely used by shielding analysts, these methods do have their limitations. Most restrictive is the requirement that the problem geometry must be one of the three basic geometries (rectangular, spherical, or cylindrical) with boundaries and material interfaces placed perpendicular to a coordinate axis. Problems with irregular boundaries and material distributions are difficult to solve accurately with the discrete-ordinates method. Also, in multidimensional geometries, the discrete-ordinates method often produces spurious oscillations in the flux densities (the *ray effect*) as an inherent consequence of the angular discretization. Finally, the discretization of the spatial and angular variables introduces numerical truncation errors, and it is necessary to use sufficiently fine angular and spatial meshes to obtain flux densities that are independent of the mesh size. For multidimensional situations in which the flux density is very anisotropic in direction and in which the medium is many mean-free-path lengths in size, typical of many shielding problems, the computational effort to obtain an accurate discrete-ordinates solution can become very large. However, unlike Monte Carlo calculations, discrete-ordinates methods can treat very deep penetration problems, i.e., the calculation of fluxes and doses at distances many mean-free-path lengths from a source.

Monte Carlo transport theory. In Monte Carlo calculations particle tracks are generated by simulating the random nature of the particle interactions with the medium. One does not even need to invoke the transport equation; all one needs are complete mathematical expressions of the probability relationships that govern the track length of an individual particle between interaction points, the choice of an interaction type at each such point, the choice of a new energy and a new directions if the interaction is of a scattering type, and the possible production of additional particles. These are all stochastic variables, and in order to make selections of specific values for these variables, one needs a complete understanding of the various processes a particle undergoes in its lifetime from the time it is given birth by the source until it is either absorbed or leaves the system under consideration.

The experience a particle undergoes from the time it leaves its source until it is absorbed or leaves the system is called its history. From such histories expected or average values about the radiation field can be estimated. For example, suppose the expected energy $\langle E \rangle$ absorbed in some small volume V in the problem geometry is being sought. There is a probability $f(E)dE$ that a particle deposits energy in dE about E. Then the expected energy deposited is simply $\langle E \rangle = \int Ef(E)dE$. Unfortunately, $f(E)$ is not known a priori and must be obtained from a transport calculation. In a Monte Carlo analysis, $f(E)$ is

constructed by scoring or tallying the energy deposited E_i in V by the ith particle history. Then in the limit of a large number of histories N

$$\langle E \rangle \equiv \int Ef(E)dE \simeq \bar{E} \equiv \frac{1}{N}\sum_{i=1}^{N} E_i . \qquad (31)$$

The process of using a computer to generate particle histories can be performed in a way completely analogous to the actual physical process of particle transport through a medium. This direct simulation of the physical transport is called an *analog* Monte Carlo procedure. However, if the tally region is far from the source regions, most analog particle histories will make zero contribution to the tally, and thus a huge number of histories must be generated to obtain a statistically meaningful result. To reduce the number of histories, *nonanalog* Monte Carlo procedures can be used whereby certain biases are introduced in the generation of particle histories to increase the chances that a particle reaches the tally region. For example, source particles could be emitted preferentially towards the tally region instead of with the usual isotropic emission. Of course, when tallying such biased histories, corrections must be made to undo the bias so that a correct score is obtained. Many biasing schemes have been developed, and are generally called variance reduction methods since, by allowing more histories to score, the statistical uncertainty or variance in the average score is reduced.

The great advantage of the Monte Carlo approach, unlike discrete-ordinates, is that it can treat complex geometries. However, Monte Carlo calculations can be computationally extremely expensive, especially for deep penetration problems. The stochastic contribution a single history makes to a particular score requires that a great many histories be simulated to achieve a good estimate of the expected or average score. If a tally region is many mean-free-path lengths from the source, very few histories reach the tally region and contribute to the score. Even with powerful variance reduction techniques, enormous numbers of histories often are required to obtain a meaningful score in deep-penetration problems.

Those readers interested in more comprehensive treatments of the Monte Carlo method will find rich resources. A number of monographs address Monte Carlo applications in radiation transport. Those designed for the specialists in nuclear reactor computations are Goertzel and Kalos (1958), Kalos (1968), Kalos et al. (1968), and Spanier and Gelbard (1969). More general treatments will be found in the books by Carter and Cashwell (1975) and Lux and Koblinger (1991). Coupled photon and electron transport are addressed in the compilation edited by Jenkins et al. (1988). A very great deal of practical information can be gleaned from the manuals for Monte Carlo computer codes. Especially recommended are those for the EGS4 code (Nelson et al. 1985), the TIGER series of codes (Halbleib et al. 1992), and the MCNP code (X-5 2003).

REFERENCES

Adams ML, Larsen EW. Fast iterative methods for discrete-ordinates particle transport calculations. Prog Nuc Energy 40:3–159; 2002.

Albert RD, Welton TA. A simplified theory of neutron attenuation and its application to reactor shield design. Pittsburgh, PA: Westinghouse Electric Corp., Atomic Power Division; WAPD-15; 1950.

Alcouffe RE, Brinkley FW, Marr D, O'Dell RD. User's guide for TWODANT: A code package for two-dimensional diffusion accelerated, neutral particle transport. Los Alamos, NM: Los Alamos National Laboratory; LA-10049-M; 1984.

Alcouffe RE, Baker RS, Brinkley FW, Marr DR, O'Dell RD, Walters WF. DANTSYS: A diffusion accelerated neutral particle transport code system. Los Alamos, NM: Los Alamos National Laboratory; LA-12969-M; 1995.

Alcouffe RE, Baker RS, Dahl JA, Turner SA. PARTISN user's guide. Los Alamos, NM: Los Alamos National Laboratory; Transport Methods Group; CCS-4; LA-UR-02-5633; 2002.

Alsmiller RG, Jr. High energy nucleon transport and space shielding. Nucl Sci Eng 27:158–189; 1967.

American Nuclear Society. American national standard gamma-ray attenuation coefficients and buildup factors for engineering materials. La Grange Park, IL: American National Standards Institute, American Nuclear Society; ANSI/ANS-6.4.3-1991; 1991.

American Nuclear Society. American national standard nuclear analysis and design of concrete radiation shielding for nuclear power plants. La Grange Park, IL: American National Standards Institute, American Nuclear Society; ANSI/ANS-6.4-1997; 1997.

Archer BR. History of the shielding of diagnostic x-ray facilities. Health Phys 69:750–758; 1995.

Archer BR, Thornby JI, Bushong SC. Diagnostic x-ray shielding design based on an empirical model of photon attenuation. Health Phys 44:507–517; 1983.

Archer BR, Conway BJ, Quinn PW. Attenuation properties of diagnostic x-ray shielding materials. Med Phys 21:1499–1507; 1994.

Barkas WH, Berger MJ. Tables of energy losses and ranges of heavy charged particles. Washington, DC: National Aeronautics and Space Administration; NASA SP-3013; 1964.

Bell MJ. ORIGEN—the Oak Ridge isotope generation and depletion code. Oak Ridge, TN: Oak Ridge National Laboratory; ORNL-4628; 1973.

Berger MJ. Reflection and transmission of gamma radiation by barriers: Monte Carlo calculation by a collision density method. J Res Nat Bur Stand 55:343; 1955.

Berger MJ. In: Proceedings of shielding symposium held at the U.S. Naval Radiological Defense Laboratory. 1956.

Berger MJ. Beta-ray dose in tissue-equivalent material immersed in a radioactive cloud. Health Phys 26:1–12; 1974.

Berger MJ, Doggett JA. Reflection and transmission of gamma radiation by barriers: Semi-analytic Monte Carlo calculation. J Res Nat Bur Stand 56:89–98; 1956.

Berger MJ, Raso DJ. Monte-Carlo calculations of gamma-ray back-scattering. Radiation Res 12:20–37; 1960.

Berger MJ, Seltzer SM. Tables of energy losses and ranges of electrons and positrons. Washington, DC: National Aeronautics and Space Administration; NASA SP-3012; 1964.

Berger MJ, Seltzer SM. Penetration of electrons and associated bremsstrahlung through aluminum targets. In: Protection against space radiation. Washington, DC: National Aeronautics and Space Administration; NASA SP-169; 1968.

Blizard EP, Abbott, LS, eds. Reactor handbook, Volume III, Part B, Shielding. New York: John Wiley and Sons; 1962.

Brockhoff RC. Calculation of albedos for neutrons and photons. Manhattan, KS: Department of Mechanical and Nuclear Engineering, Kansas State University; 2003. Dissertation.

Brockhoff RC, Shultis JK, Faw RE. Skyshine line-beam response functions for 20- to 100-MeV photons. Nucl Sci Eng 123:282–288; 1996.

Cain VR. A users manual for QAD-CG, the combinational geometry version of the QAD-P5A point kernel shielding code. San Francisco, CA: Bechtel Power Corp., Report NE007; 1977.

Cain VR, Emmett MV. BREESE-II: Auxiliary routines for implementing the albedo option in the MORSE Monte Carlo code. Oak Ridge, TN: Oak Ridge National Laboratory; ORNL/TM-6807; 1979.

Capo MA. Polynomial approximation of gamma-ray build-up data to shield design. Washington, DC: General Electric Corp., Atomic Products Division; U.S. AEC Report APEX-510; 1959.

Carlson BG. Solution of the transport equation by the Sn method. Los Alamos, NM: Los Alamos Scientific Laboratory; LA-1891; 1955.

Carlson BG, Lathrop KD. Transport theory, the method of discrete ordinates. In: Greenspan H, Kelber CN, Okrent D, eds. Computing methods in reactor physics. New York: Gordon and Breach; 1968:171–266.

Carter LL, Cashwell ED. Particle-transport simulation with the Monte Carlo method. Los Alamos NM: Los Alamos National Laboratory; Report TID-26607; 1975.

Cashwell ED, Everett CJ. A practical manual on the Monte Carlo method for random walk problems. New York: Pergamon Press; 1959.

Casper AW. Modified fast neutron attenuation functions. Cincinnati, OH: General Electric Corp., Atomic Products Div.; XDC-60-2-76; 1960.

Caswell RS, Coyne JJ, Randolph ML. Kerma factors for neutron energies below 30 MeV. Radiat Res 83:217–254; 1980.

Chandrasekhar S. Radiative transfer. Mineola, NY: Dover Publications; 1960.

Chapman GT, Storrs CL. Effective neutron removal cross sections for shielding. Oak Ridge, TN: Oak Ridge National Laboratory; ORNL-1843 (AECD-3978); 1955.

Chilton AB. A modified formula for differential exposure albedo for gamma rays reflected from concrete. Nucl Sci Eng 27:481–482; 1967.

Chilton AB. Effect of material composition on neutron penetration of concrete shields. Washington, DC: National Bureau of Standards; Report 10425; 1969.

Chilton AB. Effect of material composition on neutron penetration of concrete slabs. Washington, DC: National Bureau of Standards; Report 10425; 1971.

Chilton AB, Huddleston CM. A semi-empirical formula for differential dose albedo for gamma rays on concrete. Nucl Sci Eng 17:419–424; 1963.

Chilton AB, Davisson CM, Beach LA. Parameters for C-H albedo formula for gamma rays reflected from water, concrete, iron, and lead. Trans Am Nucl Soc 8:656; 1965.

Chilton AB, Eisenhauer CM, Simmons GL. Photon point source buildup factors for air, water, and iron. Nucl Sci Eng 73:97–107; 1980.

Coleman WA, Maerker RE, Muckenthaler FJ, Stevens PJ. Calculation of doubly differential current albedos for epicadmium neutrons incident on concrete and comparison of the subcadmium component with experiment. Nucl Sci Eng 27:411–422; 1967.

Croff AG. ORIGEN2—A revised and updated version of the Oak Ridge isotope generation and depletion code. Oak Ridge, TN: Oak Ridge National Laboratory; ORNL-5261; 1980.

Dillman LT, Von der Lage FC. Radionuclide decay schemes and nuclear parameters for use in radiation dose estimates. New York: Medical Internal Radiation Dose Committee, Society of Nuclear Medicine; Pamphlet 10; 1975.

Doggett WO, Bryan FA Jr. Theoretical dose transmission and reflection probabilities for 0.2–10.0 MeV photons obliquely incident on finite concrete barriers. Nucl Sci Eng 39:92–104; 1970.

Duderstadt JJ, Martin WR. Transport theory. New York: Wiley; 1979.

Eisenhauer CM. An engineering method for calculating protection afforded by structures against fallout radiation. Washington, DC: National Bureau of Standards; Monograph 76; 1964.

Eisenhauer CM, Simmons GL. Point isotropic buildup factors in concrete. Nucl Sci Eng 56:263–270; 1975.

England TR, Wilson WB, Stamatelatos MG. Fission product data for thermal reactors. Part 2: User's manual for EPRI-CINDER code and data. Los Alamos, NM: Los Alamos National Laboratory; LA-6746-MS (EPRI NP-356); 1976.

Engle RL, Greenborg J, Hendrickson NM. ISOSHLD—A computer code for general purpose isotope shielding analysis. Richland, WA: Battelle Northwest Laboratory; BNWL-236; 1966.

Engle WW, Jr. The users manual for ANISN: A one-dimensional discrete ordinates transport code with anisotropic scattering. Oak Ridge, TN: Oak Ridge Gaseous Diffusion Plant; Report K-1694; 1967.

Fano U, Spencer LV, Berger MJ. Penetration and diffusion of x rays. In: Encyclopedia of physics. Vol. 38, Part 2. Berlin: Springer-Verlag; 1959.

Faw RE, Shultis JK. Absorbed dose buildup factors in air for 10–100 MeV photons. Nucl Sci Eng 114:76–80; 1993.

Firestone RB, Shirley VS. Table of isotopes. New York: John Wiley and Sons; 1996.

Fournie EM, Chilton AB. Gamma-ray buildup factors for slab shields under slant incident conditions. Nucl Sci Eng 76:66–69; 1980.

French RL, Wells MB. An angular dependent albedo for fast-neutron reflection calculations. Fort Worth, TX: Radiation Research Associates, Inc.; Report RRA-M31; 1963.

Goertzel G, Kalos MH. Monte Carlo methods in transport problems. In: Progress in nuclear energy. Ser. 1, Vol. 2. New York: Pergamon Press; 1958.

Goldstein H, Wilkins JE, Jr. Calculation of the penetration of gamma rays. White Plains, NY: Nuclear Development Associates; NYO-3075; 1954.

Goldstein H. Fundamental aspects of reactor shielding. Reading, MA: Addison-Wesley; 1959.

Goldstein H. Everitt Pinell Blizard, 1916–1966. Nucl Sci Eng 27:145–150; 1967.

Gomes IC, Stevens PN. MORSE/STORM: A generalized albedo option for Monte Carlo calculations. Oak Ridge, TN: Oak Ridge National Laboratory; ORNL/FEDC-91/1; 1991.

Gopinath DV, Subbaiah KV, Trubey DK. Gamma-ray transport in a shield-tissue composite system and the buildup factor implications. Nucl Sci Eng 97:362–373; 1987.

Gui AA, Shultis JK, Faw RE. Response functions for neutron skyshine analysis. Nucl Sci Eng 125:111–127; 1997.

Haffner JW. Radiation shielding in space. New York: Academic Press; 1967.

Haggmark LG, Jones TH, Scofield NE, Gurney WJ. Differential dose rate measurements of backscattered gamma rays from concrete, aluminum, and steel. Nucl Sci Eng 23:138; 1965.

Halbleib JA, Kensek RP, Mehlhorn TA, Valdez GD, Seltzer SM, Berger MJ. ITS Version 3.0: The integrated TIGER series of coupled electron/photon Monte Carlo transport codes. Albuquerque, NM: Sandia National Laboratories; SAND91-1634; 1992.

Harima Y. An approximation of gamma-ray buildup factors by modified geometrical progression. Nucl Sci Eng 83:299–309; 1983.

Harima Y. An historical review and current status of buildup factor calculations and applications. Radiat Phys Chem 41:631–672; 1993.

Harima Y, Sakamoto Y, Tanaka S, Kawai M. Validity of the geometric-progression formula in approximating gamma-ray buildup factors. Nucl Sci Eng 94:24–35; 1986.

Harima Y, Tanaka S, Sakamoto Y, Hirayama H. Development of new gamma-ray buildup factors and applications to shielding calculations. J Nucl Sci Technol 28:74–78; 1991.

Hill TR. ONETRAN, a discrete ordinates finite element code for the solution of the one-dimensional multi group transport equation. Los Alamos, NM: Los Alamos National Laboratory; LA-5990-MS; 1975.

Hirayama H. Exposure buildup factors of high-energy gamma rays for water, concrete, iron, and lead. Nucl Technol 77:60–67; 1987.

Hubble JH. Photon cross sections, attenuation coefficients, and energy absorption coefficients from 10 keV to 100 GeV. Washington, DC: National Bureau of Standards; NSRDS-NBS 29; 1969.

Hubbell JH. Photon mass attenuation and energy-absorption coefficients from l keV to 20 MeV. Int J Appl Radiat Isotopes 33:1269–1290; 1982.

Hubbell JH, Berger MJ. Photon attenuation and energy absorption coefficients. Tabulations and discussion. Washington, DC: National Bureau of Standards; Report 8681; 1966.

Hubbell JH, Seltzer SM. Tables of x-ray mass attenuation coefficients 1 keV to 20 MeV for elements Z=1 to 92 and 48 additional substances of dosimetric interest. Gaithersburg, MD: National Institute of Standards and Technology; NISTIR 5632; 1995.

Hungerford HE. Radiation shielding in fast reactor technology, plant design. In: Yevick JG, ed. Cambridge: MIT Press; 1966.

International Commission on Radiological Protection. Radionuclide transformations. Oxford: Pergamon Press; ICRP Publication 38; Annals of the ICRP, Vols. 11–13; 1983.

International Commission on Radiological Protection. Data for use in protection against external radiation. Oxford: Pergamon Press; Publication 51, Annals of the ICRP 17, Nos. 2 & 3; 1987.

International Commission on Radiological Protection. Conversion coefficients for use in radiological protection against external radiation. Oxford: Pergamon Press; Publication 74, Annals of the ICRP 26, Nos. 3 & 4; 1996.

Jaeger RH. Engineering compendium on radiation shielding. Vol I, shielding fundamentals and methods. New York: Springer-Verlag; 1968.

Jaeger RH. Engineering compendium on radiation shielding. Vol II, shielding materials. New York: Springer-Verlag; 1975.

Jenkins TM, Nelson TM, Rindi A. Monte Carlo transport of electrons and photons. New York: Plenum Press; 1988.

Jones VC. Manhattan: The army and the atomic bomb. Washington, DC: U.S. Government Printing Office; 1985.

Kahn H. Random sampling (Monte Carlo) techniques in neutron attenuation problems, I and II. Nucleonics 6:25–37, 60–65; 1950.

Kalos MH. Monte Carlo integration of the adjoint gamma-ray transport equation. Nucl Sci Eng 33:284–290; 1968.

Kalos MH, Nakache NR, Celnik JC. Monte Carlo methods in reactor computations. In: Greenspan H, Kelber CN, Okrent D, eds. Computing methods in reactor physics. New York; Gordon and Breach; 1968.

Kocher DC. Radioactive decay tables. Washington, DC: Technical Information Center, U.S. Department of Energy; DOE/TIC 11026; 1981.

Lampley CM. The SKYSHINE-II procedure: Calculation of the effects of structure design on neutron, primary gamma-ray, and secondary gamma-ray dose rates in air. Fort Worth, TX: Radiation Research Associates; RRA-T7901; 1979.

Lampley CM, Andrews MC, Wells MB. The SKYSHINE-III procedure: Calculation of the effects of structure design on neutron, primary gamma-ray, and secondary gamma-ray dose rates in air. Fort Worth, TX: Radiation Research Associates; RRA-T8209A; 1988.

Lathrop KD. DTF-IV, a FORTRAN-IV program for solving the multigroup transport equation with anisotropic scattering. Los Alamos, NM: Los Alamos National Laboratory; LA-3373; 1965.

Lathrop KD, Brinkley FW. Theory and use of the general-geometry TWOTRAN program. Los Alamos, NM: Los Alamos National Laboratory; LA-4432; 1970.

LeDoux JC, Chilton AB. Gamma ray streaming through two-legged rectangular ducts. Nucl Sci Eng 11:362–368; 1959.

Leimdorfer M, Alsmiller RG Jr, Boughner RT. Calculations of the radiation hazards due to exposure of supersonic aircraft to solar flare protons. Nucl Sci Eng 27:151–157; 1967.

Lewis EE, Miller WF. Computational methods of neutron transport theory. New York: Wiley; 1984.

Lux I, Koblinger LK. Monte Carlo particle transport methods: Neutron and photon calculations. Boca Raton, FL: CRC Press; 1991.

Maerker RE, Muckenthaler FJ. Calculation and measurement of the fast-neutron differential dose albedo for concrete. Nucl Sci Eng 22:455–462; 1965.

Maerker RE, Muckenthaler FJ. Measurements and single-velocity calculations of differential angular thermal-neutron albedos for concrete. Nucl Sci Eng 26:339–346; 1966.

Malenfant RE. QAD: A series of point kernel general-purpose shielding programs. Los Alamos, NM: Los Alamos National Laboratory; LA-3573; 1967.

Malenfant RE. G3: A general purpose gamma-ray scattering code. Los Alamos, NM: Los Alamos National Laboratory; LA-5176; 1973. Available from RSICC as CCC-564/G33-GP; 1990.

Martin MJ. Nuclear decay data for selected radionuclides. Oak Ridge, TN: Oak Ridge National Laboratory; ORNL-5114; 1976.

Martin MJ, Blichert-Toft PH. Radioactive atoms, Auger electrons, alpha, beta, gamma, and x-ray data. Nuclear Data Tables Part A, Vol. 8, Nos. 1&2; 1970.

McGinley PH, Miner MS. A history of radiation shielding of x-ray therapy rooms. Health Phys 69:759–765; 1995.

Morris EE, Chilton AB, Vetter AF. Tabulation and empirical representation of infinite-medium gamma-ray buildup factors for monoenergetic point isotropic sources in water, aluminum, and concrete. Nucl Sci Eng 56:171–178; 1975.

Mutscheller A. Physical standards of protection against Roentgen-ray dangers. Am J Roentgenol Radiat Therapy 13:65–70; 1925.

Mynatt FR, Rhoades WA. DOT III two-dimensional discrete ordinates transport code. Oak Ridge, TN: Oak Ridge National Laboratory; ORNL-TM-4280; 1973.

Mynatt FR, Muckenthaler FJ, Stevens PN. Development of two-dimensional discrete ordinates transport theory for radiation shielding. Oak Ridge, TN: Union Carbide Corporation; USAEC Report CTC-INF-52; 1969.

National Council on Radiation Protection and Measurements. X-ray protection. Washington, DC: NCRP; NBS Handbook 15, NCRP Report No. 1; 1931.

National Council on Radiation Protection and Measurements. Radium protection for amounts up to 300 mg. Washington, DC: NCRP; NBS Handbook 18, NCRP Report No. 2; 1934.

National Council on Radiation Protection and Measurements. X-ray protection. Washington, DC: NCRP; NBS Handbook 20, NCRP Report No. 3; 1936.

National Council on Radiation Protection and Measurements. Radium protection. Washington, DC: NCRP; NBS Handbook 23, NCRP Report No. 4; 1938.

National Council on Radiation Protection and Measurements. Safe handling of radioactive luminous compounds. Washington, DC: NCRP; NBS Handbook 27; NCRP Report No. 5; 1941.

National Council on Radiation Protection and Measurements. Protection against neutron radiation. Washington, DC: NCRP; Report 38; 1971.

National Council on Radiation Protection and Measurements. Structural shielding design and evaluation for medical use of x-rays and gamma rays of energies up to 10 MeV. Washington, DC: NCRP; Report 49; 1976.

National Council on Radiation Protection and Measurements. Radiation protection for particle accelerator facilities. Washington, DC: NCRP; Report 144; 2003.

Negin CA. The microskyshine manual. Rockville, MD: Grove Engineering; 1987.

Negin CA, Worku G. Microshield v. 5 user's manual. Rockville, MD: Grove Engineering; 1998.

Nelson WR, Hirayama H, Rogers DWO. The EGS4 code system. Menlo Park, CA: Stanford Linear Accelerator Center; SLAC-265; 1985.

O'Dell RD, Brinkley FW Jr., Marr D. User's manual for ONEDANT: A code package for one-dimensional diffusion accelerated, neutral particle transport. Los Alamos, NM: Los Alamos National Laboratory; LA-9184-M; 1982.

Plechaty EF. Cullen DE, Howerton RJ. Tables and graphs of photon-interaction cross sections from 0.1 keV to 100 MeV derived from the LLL evaluated-nuclear-data library. Livermore, CA: Lawrence Livermore National Laboratory; Report UCRL-50400, Vol. 6, Rev. 3; 1981.

Price BT, Horton CC, Spinney KT. Radiation shielding. New York: The Macmillan Co.; 1957.

Price JH, Blattner WGM. Utilization instructions for QADMOD-G. Fort Worth, TX: Radiation Research Assoc., Inc.; RRA-N7914; 1979. Available from RSICC as CCC565/QADMOD-GP.

Raso DJ. Monte Carlo calculations on the reflection and transmission of scattered gamma rays. Nucl Sci Eng 17:411–420; 1963.

Rhoades WA, Childs RL. The TORT three-dimensional discrete ordinates neutron/photon transport code. Oak Ridge, TN: Oak Ridge National Laboratory; ORNL-6268; 1987.

Rhoades WA, Simpson DB. The TORT three-dimensional discrete ordinates neutron/photon transport code. Oak Ridge, TN: Oak Ridge National Laboratory; ORNL/TM-13221; 1997.

Rhoades WA, Simson DB, Childs RL, Engle WW Jr. The DOT-IV two-dimensional discrete ordinates transport code with space-dependent mesh and quadrature. Oak Ridge, TN: Oak Ridge National Laboratory; ORNL/TM-6529; 1979.

Rockwell T, III. Reactor shielding design manual. Princeton, NJ: D. Van Nostrand; 1956.

Rockwell T. Creating the new world—Stories and images from the dawn of the atomic age. Bloomington, IN: 1st Books Library; 2004.

Roussin RW, Schmidt FAR. Adjoint Sn calculations of coupled neutron and gamma-ray transport through concrete slabs. Nucl Eng Design 15:319–343; 1971.

Roussin RW, Alsmiller RG Jr, Barish J. Calculations of the transport of neutrons and secondary gamma rays through concrete for incident neutrons in the energy range 15 to 75 MeV. Nucl Eng Design 24:250–257; 1973.

Schaeffer NM. Historical background. In: Schaeffer NM, ed. Reactor shielding. Washington, DC: U.S. Atomic Energy Commission; TID-25951; 1973.

Selph WE. Albedos, ducts, and voids. In: Schaeffer NM, ed. Reactor shielding. Washington, DC: U.S. Atomic Energy Commission; TID-25951; 1973.

Seltzer SM. Calculation of photon mass energy-transfer and energy-absorption coefficients. Radiat Res 136:147–179; 1993.

Shultis JK, Faw RE. Radiation shielding. La Grange Park, IL: American Nuclear Society; 2000.

Shultis JK, Faw RE, Bassett MS. The integral line-beam method for gamma skyshine analysis. Nucl Sci Eng 107:228–245; 1991.

Shure K. P-3 multigroup calculations of neutron attenuation. Nucl Sci Eng 19:310–320; 1964.

Simmons GL. An adjoint gamma-ray moments computer code, ADJMOM-1. Washington, DC: National Bureau of Standards; NBS Technical Note 748; 1973.

Simmons GL, Albert TE, Gritzner DM. The SAI/EPRI information library. La Jolla, CA: Science Applications Inc.; Report SAI-013-79-525-LJ; 1979.

Simpkin DJ. Shielding requirements for mammography. Health Phys 53:267–279; 1987.

Simpkin DJ. Shielding requirements for constant-potential diagnostic x-ray beams determined by a Monte Carlo calculation. Health Phys 56:151–154; 1989.

Simpkin DJ. Transmission data for shielding diagnostic x-ray facilities. Health Phys 68:704–709; 1995.

Simpson JW. Nuclear power from underseas to outer space. La Grange Park, IL: American Nuclear Society; 1995.

Song YT, Huddleston CM, Chilton AB. Differential dose albedo for fast neutrons. Nucl Sci Eng 35:401–405; 1969.
Spanier J, Gelbard EM. Monte Carlo principles and neutron transport problems. Reading, MA: Addison-Wesley; 1969.
Spencer LV. Structure shielding against fallout radiation from nuclear weapons. Washington, DC: National Bureau of Standards; Monograph 42; 1962.
Spencer LV, Fano U. Penetration and diffusion of x-rays: calculation of spatial distributions by polynomial expansion. J Res Nat Bur Stds 46:446; 1951.
Spencer LV, Chilton AB, Eisenhauer CM. Structure shielding against fallout gamma rays from nuclear detonations. Washington, DC: National Bureau of Standards, U.S. Government Printing Office; Special Publication 570; 1980.
Stedry MH. A Monte Carlo line-beam calculation of gamma-ray skyshine for shielded sources. Manhattan, KS: Kansas State University; 1994. Thesis.
Storm E, Israel HI. Photon cross sections from 1 keV to 100 MeV for elements Z=1 to Z=100. Nucl Data Tables A 7:565–681; 1967.
Straker EA, Stevens PN, Irving DC, Cain VR. MORSE code: A multi group neutron and gamma-ray Monte Carlo transport code. Oak Ridge, TN: Oak Ridge National Laboratory; ORNL-4585; 1970.
Subbaiah KV, Natarajan A, Gopinath DV, Trubey DK. Effect of fluorescence, bremsstrahlung, and annihilation radiation in the spectra and energy deposition of gamma rays in bulk media. Nucl Sci Eng 81:172–195; 1982.
Takeuchi K, Tanaka S. Buildup factors of gamma rays, including bremsstrahlung and annihilation radiation for water, concrete, iron, and lead. Nucl Sci Eng 87:478–489; 1984.
Takeuchi K, Tanaka S, Kinno M. Transport calculation of gamma rays including bremsstrahlung by the discrete ordinates code PALLAS. Nucl Sci Eng 78:273–283; 1981.
Tanaka S, Takeuchi K. Detailed investigation of the buildup factors and spectra for point isotropic gamma ray sources in the vicinity of the K edge in lead. Nucl Sci Eng 93:376–385; 1986.
Taylor JJ. Application of gamma-ray buildup data to shield design. Washington DC: Westinghouse Electric Corporation, Atomic Power Division; USAEC Report WAPD-RM-217; 1954.
Taylor LS. Organization for radiation protection: The operation of the ICRP and NCRP, 1928–1974. Washington, DC: U.S. Department of Energy; 1979.
Taylor LS. The development of radiation protection standards (1925–1940). Health Phys 41:227–232; 1981.
Wang X, Faw RE. Transmission of neutrons and secondary gamma rays through concrete slabs. Radiat Protect Dosim 60:212–222; 1995.
Weber DA, Eckerman KE, Dillman LT, Ryman JC. MIRD: Radionuclide data and decay schemes. New York: Medical Internal Radiation Dose Committee, Society of Nuclear Medicine; 1989.
Wells MB. Reflection of thermal neutrons and neutron capture gamma rays from concrete. Fort Worth, TX: Radiation Research Associates, Inc.; U.S. AEC Report RRA-M44; 1964.
White JE, Ingersoll DT, Wright RQ, Hunter HT, Slater CO, Greene NM, MacFarlane RE, Roussin RW. Production and testing of the revised VITAMIN-B6 fine-group and the BUGLE-96 broad-group neutron/photon cross-section libraries derived from ENDF/B-VI.3 nuclear data. Oak Ridge, TN: Oak Ridge National Laboratory; ORNL-6795 (NUREG/CR-6214), Rev. 1; 1995.
Wyckoff JM, Chilton AB. Dose due to practical neutron energy distributions incident on concrete shielding slabs. La Grange Park, IL: IRPA; Proceedings of the 3rd International Congress IRPA, American Nuclear Society; 1973.
X-5 Monte Carlo Team. MCNP—a general Monte Carlo n-particle transport code, version 5. Los Alamos, NM: Los Alamos National Laboratory; LA-UR-03-1987 (Vol. I: Overview and theory); LA-UR-03-0245 (Vol. II: User's guide); 2003.
Zerby CD, Keller FL. Electron transport theory, calculations, and experiments. Nucl Sci Eng 27:190–218; 1967.

■ ■